UNIVERSITÀ DEGLI STUDI DI PADOVA
Dipartimento di Ingegneria Industriale DII
Corso di laurea magistrale in Energy Engineering

Residential users with load shifting and comfort evaluation, the economic advantage and their role in energy communities

Supervisors: Andrea Lazzaretto
Sotirios Karellas
Gianluca Carraro
Enrico Dal Cin
Konstantinos Braimakis

Student: Giacomo Olivan

Academic year: 2022/2023

Index

Abstract

The work carried out in this thesis is set to develop a model aiming to provide an optimized design and operation of a residential user with the ability of shifting in time a part of the electrical and thermal load, while evaluating the comfort of the user as a limit to the load shifting. Consequently, the primary objective of this research is to assess the efficacy of the model, quantify the savings resulting from its implementation, and scrutinize its performance within the context of Energy Communities. This model is subsequently subjected to a comparative analysis alongside two basic types of Demand Response: Price-Based and Incentive-Based. This comparative evaluation aims to determine the economic feasibility of this form of Demand Response, in contrast to a simplified alternative. In this analysis, the model achieves a 26% reduction in yearly costs compared to a base case, where all the electricity is bought from the grid and the heat is generated with a natural gas boiler. Meanwhile, the Incentive Based and the Price Based respectively achieve a 17% and a 19% reduction from the base case.
As the analysis' results show, this form of Demand Response demonstrates a clear economic advantage, prompting its integration into various Energy Community settings for the exploration of potential additional savings, as the capability of load shifting could benefit the Energy Community.
An indicator is employed to gauge the cost relative to the amount of energy utilized - the cost of energy. For the single residential household this cost of energy amounts to 25.83 $\frac{c€}{kWh}$ when only the electrical demand is considered and 19.65 $\frac{c€}{kWh}$ when the thermal demand is also considered. As for the optimized design, the installed capacities for the single household comprise 2.28 kW of photovoltaic panels, 3.13 kW of heat pump, 1.02 kWh of thermal energy storage and 1.41 kWh of electrical energy storage.
This model is then incorporated into an energy community. First, a community of all single household with load shifting is tested and the resulting trend for the cost of energy - population curve shows an almost flat trend, with the cost of energy remaining stable. Next, an energy community composed of residential users with and without load shifting is tested, and as the number of users without load shifting increases, the cost of energy increased as well, independently of the number of users with load shifting. Consequently an industrial user is introduced, and the energy community is tested first with only users with load shifting and then with a mix of users with and without load shifting. In both scenarios, the cost of energy remains below that of a single household, but exceeds that of the industrial user operating alone. Therefore, the findings indicate that the model as is does not justify the formation of an energy community from an economic perspective.
In conclusion, a model of a single residential household is developed. The model offers an optimized design and operation, while evaluating both the electrical and thermal comfort of the household. The possibility of load shifting is therefore limited by a threshold given by the user. Even with this limitation, the model is able to provide savings to the user, proving to be economically viable.

Sommario

Il lavoro svolto in questa tesi si propone di sviluppare un modello volto a fornire una progettazione e un funzionamento ottimizzati per un utente residenziale con la capacità di spostare nel tempo una parte del carico elettrico e termico, valutando nel contempo il comfort dell'utente come limite allo spostamento del carico. Di conseguenza, l'obiettivo principale di questa ricerca è valutare l'efficacia del modello, quantificare i risparmi derivanti dalla sua implementazione e analizzarne le prestazioni nel contesto delle Comunità Energetiche. Questo modello è successivamente sottoposto a un'analisi comparativa insieme a due tipi fondamentali di Demand Response: uno basato sul prezzo e uno basato sugli incentivi. Questa valutazione comparativa mira a determinare la fattibilità economica di questa forma di Demand Response, in contrasto con un'alternativa semplificata. In questa analisi, il modello ottiene una riduzione del 26% dei costi annuali rispetto allo scenario di base, dove tutta l'elettricità è comprata dalla rete ed il calore è prodotto da una caldaia a gas naturale. Invece, il modello basato sugli incentivi e quello basato sul prezzo ottengono rispettivamente una riduzione del 17% e il 19% rispetto al caso base.
Come mostrano i risultati dell'analisi, questa forma di Demand Response presenta un chiaro vantaggio economico, favorendo la sua integrazione in varie configurazioni di Comunità Energetiche per l'esplorazione di potenziali risparmi aggiuntivi, poiché la capacità di spostamento del carico potrebbe beneficiare la Comunità Energetica.
Un indicatore viene impiegato per valutare il costo in rapporto alla quantità di energia utilizzata - il costo dell'energia. Per la singola abitazione il costo dell'energia è pari a 25,83 $\frac{c€}{kWh}$ se si considera solo la domanda elettrica e a 19,65 $\frac{c€}{kWh}$ se si considera anche la domanda termica. Per quanto riguarda l'ottimizzazione del design, le capacità installate per la singola abitazione comprendono 2,28 kW di pannelli fotovoltaici, 3,13 kW di pompa di calore, 1,02 kWh di accumulo di energia termica e 1,41 kWh di accumulo di energia elettrica.
Questo modello è quindi incorporato in una comunità energetica. Dapprima viene testata una comunità composta di sole abitazioni con load shifting e la tendenza risultante per la curva costo dell'energia - popolazione mostra un andamento quasi piatto, con il costo dell'energia che rimane stabile. Successivamente, viene testata una comunità energetica composta da utenti residenziali con e senza load shifting, e all'aumentare del numero di utenti senza load shifting aumenta anche il costo dell'energia, indipendentemente dal numero di utenti con load shifting. Successivamente viene introdotto un utente industriale e la comunità energetica viene testata prima solo con utenti con load shifting e poi con un mix di utenti con e senza load shifting. In entrambi i casi, il costo dell'energia rimane inferiore a quello di un'unica abitazione, ma supera quello dell'utente industriale operante da solo.Di conseguenza, i risultati indicano che il modello attualmente non giustifica la formazione di una comunità energetica da un punto di vista economico.
In conclusione, è stato sviluppato un modello di singola abitazione residenziale. Il modello offre una progettazione e un operazione ottimizzati, valutando al contempo il comfort elettrico e termico dell'abitazione. La possibilità di spostare il carico è quindi limitata da una soglia indicata dall'utente. Anche con questa limitazione, il modello è in grado di fornire risparmi all'utente, dimostrandosi economicamente vantaggioso.

Nomenclature

A	area
C	capacity
Cap	capacity
c_{buy}	buying price
COP	coefficient of performance
c_p	specific heat capacity
$csell$	selling price
EER	energy efficiency ratio
η	efficiency
f_{sol}	solar radiation absorption fraction
$f_{heat,rad}$	radiative heating fraction
h_A	external wall heat transfer coefficient
h_f	solar absorptivity on wall exterior
λ	thermal conductivity
n	air circulations
$O\&M$	operation and maintenance
occ	occupancy
P	power, population
Φ	heat flux
Q	thermal energy
R	resistance
ρ	density
sd	self discharge
SOC	state of charge
$SolRad$	solar radiation
T	temperature
ToU	time of use
trg	target
V	volume

Subscripts

amb	ambient
com	comfort
$dish$	dishwasher
$drye$	dryer
el	electrical, electricity
exp	exported
imp	imported
int	internal
INV	investment
OP	operation
th	thermal
$wash$	washer

Abbreviations

AC	air conditioning
CA	controllable appliance
COE	cost of energy
DHW	domestic hot water
DR	demand response
DSM	demand side management
EC	energy community
EES	electrical energy storage
HP	heat pump
$IBDR$	incentive based demand response
$PBDR$	price based demand response
PV	photovoltaic panels
SA	shiftable appliance
TES	thermal energy storage

1) Introduction

Global efforts are underway to limit greenhouse gas (GHG) emissions in response to the urgent necessity of action on the problem of global warming and climate change. These initiatives are driven by the necessity for timely interventions to effectively curb GHG emissions, aligning with the objectives outlined in the Paris Agreement of 2015 [1]. The primary goal of these endeavors is to ensure that the rise in global temperatures remains well below the 2°C threshold by the end of this century. To ensure action the European Union (EU) passed legislation to establish objectives and the subsequent road-map to reach them. With the "Clean energy for all Europeans" [2] and "Fit for 55" [3] packages the two main set targets are the reduction of GHG emissions of 55% by 2030 and carbon neutrality by 2050. Furthermore, a significant part of these directives are directed towards the electricity sector, responsible for emitting 13 gigatonnes of carbon dioxide (Gt CO_2) in 2021. This sector alone accounts for more than one-third of the world's energy-related CO_2 emissions.

1.1 Energy Communities

In this context, a concept of an "Energy Community" (EC) has been gaining traction. The possibility for local energy users to aggregate, leading to better usage of energy, to economical benefits for the users and better exploitation of renewable energy sources (RES). In the European context two types of ECs are defined, through the Renewable Energy Directive (RED II) [4], the Citizen and Renewable Energy Community (respectively CEC and REC). In [5], the author summarises the definition of an EC as "legal entities based on the voluntary participation of residential users, small and medium sized enterprises (SMEs) and local authorities, with the main purpose of providing environmental, economic or social benefits rather than attaining financial profits".But a distinction between the CEC and the REC is present. First the REC can only exploit RES, but can satisfy different types of energy demands (such as thermal, electric, etc.). Instead the CEC only manages the electricity demand, but can utilized both renewable and fossil-based sources.

1.2 Demand Response

Another important strategy to better exploit RES and reduce waste are the Demand Response (DR) strategies, also called Demand Side Management (DSM) techniques. These strategies consist in deploying a series of reductions of a load in response to a signal from the EC, usually associated with high demand within the EC. The most common type of DR regards the use of electricity and adjusting a user's demand to minimize costs during periods characterized by elevated electricity prices. When the overall load is not reduced but only varied in the time component, it is called load-shifting. DSM and load-shifting are both proven to be both economically and energetically viable, within and without ECs [5] [6] [7] [8].

1.3 Application of Demand Response to residential users

The focus of this thesis is the application of Demand Response (DR) strategies to residential users. In particular, DR is applied to a characterized load for the household, allowing a degree of load shifting. However, to limit in time and magnitude the load shifting for both the electrical and thermal loads, a level of comfort is defined for both types of loads and characterized for the user.
This approach has already proven to be effective and economically viable, as can be seen in [9], [10], [11].

1.4 Literature Review

1.4.1 Demand Response

In [8] Dal Cin et al. analyzed the potential of DR in an ECs, showing a decrease in both costs and emissions. Furthermore, the application of DR upstream of the design problem allowed for better deployment of renewable sources.
Volpato et al., in [12] put price-based DR (PBDR) and incentive-based DR (IBDR) under a comparative analysis with different users composing an EC. In all cases both DR types lead to savings, in particular the PBDR allows up to 50% savings in a REC.
The inclusion of DR even in micro-grids allows to reduce costs and emissions, as shown in [6], even considering uncertainties from day-ahead scheduling.
Fan et al. research an algorithm capable of scheduling different appliances in a smart residential community in [13]. The user's data is gathered in two blocks: the appliance data in aggregated form to lower privacy problems and a target price set by the user. This results in an optimization of the user's surplus with positive impact on the overall community.
A design and operation optimization is performed by Luo et al. [14], where the characterization of the user's load coupled with DR permitted a decrease in peak electrical power of 56% even under a trigeneration setting.

1.4.2 User comfort

Another important factor in DR is user behaviour, as more savings can be obtained with appropriate energetic behaviour from the user, as shown in [7]. As users lowered their loads by decreasing the lights usage by 20%, the savings went from 10% and 19% for a simple Photovoltaic panels (PV)-Electric Energy Storage (EES) system to 20% and 27% with a behaviour change.
Ghilardi et al. in [15] perform an analysis of multi-energy system overseeing multiple buildings with district heating and show that applying a comfort and occupancy based thermal comfort strategy leads to savings up to 74% in some cases, but positive savings in all cases.
In [16] the author proposes a formulation to estimate user comfort loss due to automated DR, showing feasibility in solving a DR problem while accounting for comfort of the user.
Alıç et al. research in [10] a Home Energy Management System (HEMS) with the objective of minimizing both the consumer's cost and the daily discomfort. Using a Montecarlo simulation they obtain a Pareto front of solutions, since the objective are contrasting. This study shows the possibility of achieving good savings, with around a dollar of saving per day, even under the maximum comfort.
In [11] Yang et al. perform an analysis on a Integrated Energy System (IES) considering DR and thermal comfort. They simulate three cases: the first without DR and thermal comfort being considered in design and operation, the second with only DR and the third with both being considered. The second case already introduces savings (around 4.5% compared to the base case), but in the third case the savings are even higher (around 6.7%) with low comfort loss for the user.

1.4.3 Installed systems

In [17], Wu et al. study the design and operation problem of a near-zero EC. They find that PV is the best contributor to EC energy demand and that there is potential for near-zero ECs.
Aruta et al. in [18], perform an analysis on the possible renovation of social housing, to turn it into an EC using PV and EES. The results show both economical and environmental benefits in the retrofit operation.
Overall the application of DR is proven to be effective, but lacks either its integration with the design optimization, a good characterization of the user's load or a definition of either comfort.

1.5 Novelty and Goal

Energy communities have been subjects of research across various points of view. Studies have delved into optimizing their design and operation, investigating Demand Response mechanisms, exploring residential users characterized by their load patterns, scrutinizing load-shifting strategies, and assessing user comfort within this framework. However, the novelty presented in this work lies in the amalgamation of these elements, which, while individually examined, have seldom been collectively explored. Such as: the optimization of an energy community design and operation, including different types of users and residential users having a characterized load that allows load shifting with their comfort being evaluated and given as a constraint to the model.
In this thesis it is proposed a model to study an energy community with the residential users having a characterized electrical load with three types of appliances being shiftable. The thermal load is derived from a electric circuit equivalent model, allowing the heating to be controllable. The overall comfort of a user is then characterized and is set as a limit. The goals outlined for this work are:

- Develop a model capable of simulating an energy community under constraints of optimal design and operation.
- Implement DSM strategies for the residential users, enabling the shifting of loads and characterize the loss of electrical and thermal comfort of the user.
- Quantify the savings generated from the implementation of DSM and verify the correlation between savings and loss of comfort of the user.
- Evaluate the performance of the model when integrated within an EC.

Table 1 presents a comparison of articles analyzed for this work, specifically focusing on modeling aspects under consideration. Each entry in the table indicates whether a particular aspect of analysis is addressed in the respective article.

Reference	System design optimization	System operation optimization	Demand Response	Residential electric load characterization	Electrical comfort	Thermal comfort
[17]	✓	✓				
[18]	✓	✓				
[19]	✓	✓				
[20]	✓	✓				
[6]		✓	✓			
[12]		✓	✓			
[21]		✓	✓			
[15]		✓				✓
[8]	✓	✓	✓			
[16]			✓	✓	✓	
[13]			✓	✓	✓	
[14]	✓	✓	✓	✓		
[9]		✓	✓	✓	✓	
[5]		✓	✓	✓	✓	✓
[10]		✓	✓	✓	✓	✓
[22]		✓	✓	✓	✓	✓
[11]	✓	✓	✓	✓		✓
Proposed work	✓	✓	✓	✓	✓	✓

Table 1: Comparison of articles within the EC-related literature that focus on the modeling aspects under consideration.

2) Method

In this chapter, the fundamental components of the model, including data, variables, and equations, are delineated. Subsequently, the DSM strategies are examined and an optimizer based strategy is proposed. The concluding section lists the analyses conducted to reach the objectives.
The model is implemented in Python and solved using the Gurobi optimizer. A brief summary of the fundamental informations about the model is supplied hereafter:

- The model operates under a Time of Use (ToU) tariff.
- The electrical energy is generated only from photovoltaic panels (PV) and a electrical energy storage (EES) is possible.
- The thermal energy is generated only from a heat pump (HP) and a thermal energy storage (TES) is possible.
- When loads are shifted a loss of comfort happens, which is characterized differently for electrical and thermal loads and a comfort level is set and utilized as a boundary to the load shifting.

2.1 Inputs

The inputs or initial data for our model can be categorized into four distinct classes: Geographical and techno-economical data, data pertaining to the energy generation, to the energy storages and to the single household.

2.1.1 Geographical and Techno-Economical data

Solar radiation and meteorological data were sourced from the European PVGIS platform. The dataset is structured for four representative days (denoted as k in 1, ..., K, where $K = 4$), each corresponding to a season. Furthermore, the dataset is divided into 24-hour intervals (denoted as h in 1, ..., H, where $H = 24$), resulting in a matrix with dimensions H by K, specifically 24 by 4.
The data for this category is:

- Solar Radiation $[W/m^2]$
- Ambient Temperature [°C]
- Electricity Prices [€/MWh]
- Occupancy of the Household (binary value) [-]

Additionally some weights are given to each typical day, representing how many of each days of the respective season are present in a year. The weights are: (91, 92, 91, 91). Another important parameter for the economical analysis is the interest rate, which is set at 5%.

2.1.2 Generators data

In the model only two generators are taken into account, each dedicated to a specific type of energy. Photovoltaic panels (PV) are adopted for electricity generation, while a heat pump (HP) is considered for heat production.
For the PV the following characteristics are defined:

	Unit	Value
Investment Costs	€/kWp	1250
O&M Costs	% Inv./yr	1.1
Lifetime	yr	20

Table 2: PV Characteristics

For the HP the following characteristics are defined:

	Unit	Value
Investment Costs	€/kWth	1500
O&M Costs	% Inv./yr	2.8
Lifetime	yr	20
Minimum Load	% Cap.	10
Linearization Coeff. variable	-	1.214
Linearization Coeff. fixed	-	0.312

Table 3: HP Characteristics

For the air conditioning (AC) the following characteristics are defined:

	Unit	Value
Investment Costs	€/kWth	1500
O&M Costs	% Inv./yr	2.8
Lifetime	yr	20
Minimum Load	% Cap.	10
Linearization Coeff. variable	-	1.214
Linearization Coeff. fixed	-	0.312

Table 4: AC Characteristics

2.1.3 Energy storages data

For each type of generator a storage is considered: an Electrical Energy Storage (EES) and a Thermal Energy Storage (TES). For the EES the following characteristics are defined:

	Unit	Value
Investment Costs	€/kWh	1500
O&M Costs	% Inv./yr	1
Lifetime	yr	20
Round-trip Efficiency	%	91
Self Discharge	% SOC/hr	0.04
Output Capacity	kW/kWh	3
Input Capacity	kW/kWh	0.5

Table 5: EES Characteristics

For the TES the following characteristics are defined:

	Unit	Value
Investment Costs	€/kWh	400
O&M Costs	% Inv./yr	4
Lifetime	yr	20
Round-trip Efficiency	%	98
Self Discharge	% SOC/hr	2.1
Output Capacity	kW/kWh	0.7
Input Capacity	kW/kWh	0.7

Table 6: TES Characteristics

2.1.4 Household data

This section data regarding the calculations of electrical and thermal load characteristics is contained. Three appliances were selected for the DSM, as they offer the best combination of power and flexibility [23], listed hereafter: The target time listed in the table is the

	Rated Power [kW]	Run time [h]	Target time [h]
Washing Machine	2.2	2	22
Dish Washer	1.2	1	21
Dryer	2.5	1	8

Table 7: Electrical Load Characteristics

preferred start time of the respective appliance expressed by the user.
In the following table, the data employed to formulate the thermal load of the residential user is detailed. The coefficient $f_{heat,rad}$ is extracted from [24], the coefficients f_{sol} and h_f are derived from [25] and the coefficient h_A is taken from [26].

	Unit	Value
V_{DHW}	L/day	150
T_{out}	°C	50
T_{in}	°C	15
$T_{target,heating}$	°C	20
$T_{target,cooling}$	°C	26
$T_{variation}$	°C	3
$f_{heat,rad}$	-	0.75
f_{sol}	-	0.3
h_f	-	0.2
h_A	$W/m^2 \cdot K$	6
L_1	m	20
L_2	m	7
h	m	2.7
n	h^{-1}	0.3

Table 8: Thermal Load Characteristics

Hereafter the characteristics of the wall's components are listed, taken from [25]. The structure of the wall is set to be CMIMC.

	Coating (C)	Masonry (M)	Insulation (I)
Size [cm]	2	18	4
λ $[W/m \cdot K]$	0.87	0.52	0.04
ρ $[kg/m^3]$	1900	1200	16
c_p $[W/kg \cdot K]$	1000	800	1200

Table 9: Household's Wall Characteristics

2.2 Model

The mathematical framework of the model is introduced in this section, outlining its variables, objective function, and constraints.

2.2.1 Variables

In this section, a list of the model's variables is provided, specifying whether they are decision or dependent variables, their dimensions (which can range up to 25 (H+1) by 4 (K) by the number of houses in the community (P)), and their respective units of measurement.

PV

Decision variables:

- Capacity, Cap_{PV} [kWp] - Size: 1

Dependent variables:

- Produced power, P_{PV} [kW] - Size: [H, K]

HP

Decision variables:

- Capacity, Cap_{HP} [kWth] - Size: [P]
- Output heat, Q_{HP} [kW] - Size: [H, K, P]
- On/off status, δ_{HP} [-] - Size: [H, K, P]
- Auxiliary variable, θ_{HP} [-] - Size: [H, K, P]

Dependent variables:

- Power consumption, P_{HP} [kW] - Size: [H, K, P]

AC

Decision variables:

- Capacity, Cap_{AC} [kWth] - Size: [P]
- Output cold, Q_{AC} [kW] - Size: [H, K, P]
- On/off status, δ_{AC} [-] - Size: [H, K, P]
- Auxiliary variable, θ_{AC} [-] - Size: [H, K, P]

Dependent variables:

- Power consumption, P_{AC} [kW] - Size: [H, K, P]

EES

Decision variables:

- Capacity, Cap_{EES} [kW] - Size: 1
- State of Charge, SOC_{EES} [-] - Size: [H+1, K]
- Charging power, $P_{c,EES}$ [kW] - Size: [H, K]
- Discharging power, $P_{d,EES}$ [kW] - Size: [H, K]
- Binary value for charging/discharging, δ_{EES} [-] - Size: [H, K]
- Auxiliary variable for charge, $\theta_{c,EES}$ [-] - Size: [H, K]
- Auxiliary variable for discharge, $\theta_{d,EES}$ [-] - Size: [H, K]

TES

Decision variables:

- Capacity, Cap_{TES} [kW] - Size: [P]
- State of Charge, SOC_{TES} [-] - Size: [H+1, K, P]
- Charging heat, $P_{c,TES}$ [kW] - Size: [H, K, P]

- Discharging heat, $P_{d,TES}$ [kW] - Size: [H, K, P]
- Binary value for charging/discharging, δ_{TES} [-] - Size: [H, K, P]
- Auxiliary variable for charge, $\theta_{c,TES}$ [-] - Size: [H, K, P]
- Auxiliary variable for discharge, $\theta_{d,TES}$ [-] - Size: [H, K, P]

Power exchanges with the grid

Decision variables:

- Imported power, P_{imp} [kW] - Size: [H, K]
- Exported power, P_{exp} [kW] - Size: [H, K]

House electricity load

Decision variables:

- Washing machine power consumption, P_{wash} [kW] - Size: [H+1, K, P]
- On/off status washing machine, δ_{wash} [-] - Size: [H, K, P]
- Dish washer power consumption, P_{dish} [kW] - Size: [H, K, P]
- On/off status dish washer, δ_{dish} [-] - Size: [H, K, P]
- Dryer power consumption, P_{drye} [kW] - Size: [H, K, P]
- On/off status dryer, δ_{drye} [-] - Size: [H, K, P]

Dependent variables:

- Electricity demand, Dem_{El} [kW] - Size: [H, K]

House heating load

Decision variables:

- Heating demand, Φ_h [kW] - Size: [H, K, P]
- Cooling demand, Φ_c [kW] - Size: [H, K, P]
- Internal temperature, T_{int} [°C] - Size: [H, K, P]
- Wall temperature, T_w [°C] - Size: [H, K, P]

Dependent variables:

- Thermal energy demand, Dem_{Th} [kW] - Size: [H, K, P]
- Air heating fraction, $\Phi_{h,air}$ [kW] - Size: [H, K, P]
- Walls heating fraction, $\Phi_{h,wall}$ [kW] - Size: [H, K, P]

2.2.2 Objective function

The objective function is the end goal of the model, and in this work the economic optimization is the main focus. So, the chosen objective function is the minimization of the yearly cost for the whole community.
The cost is divided into two components: investments and operation. The equations are of the components are the following:

$$\begin{aligned} Cost_{INV} = & \left(\frac{r\cdot(1+r)^{n_{PV}}}{(1+r)^{n_{PV}}-1} + O\&M_{PV}\right)\cdot inv_{PV}\cdot Cap_{PV} + \\ & \left(\frac{r\cdot(1+r)^{n_{HP}}}{(1+r)^{n_{HP}}-1} + O\&M_{HP}\right)\cdot inv_{HP}\cdot \sum_{i=0}^{P} Cap_{HP,i} + \\ & \left(\frac{r\cdot(1+r)^{n_{AC}}}{(1+r)^{n_{AC}}-1} + O\&M_{AC}\right)\cdot inv_{AC}\cdot \sum_{i=0}^{P} Cap_{AC,i} + \\ & \left(\frac{r\cdot(1+r)^{n_{EES}}}{(1+r)^{n_{EES}}-1} + O\&M_{EES}\right)\cdot inv_{EES}\cdot Cap_{EES} + \\ & \left(\frac{r\cdot(1+r)^{n_{TES}}}{(1+r)^{n_{TES}}-1} + O\&M_{TES}\right)\cdot inv_{TES}\cdot \sum_{i=0}^{P} Cap_{TES,i} \end{aligned} \tag{1}$$

The investment cost is actualized and subdivided equally for each year. The investment costs also includes the O&M as they are defined as a fraction of the investment. The operation costs are then only the difference between the cost of imported electricity and the revenue of sold electricity.

$$Cost_{OP} = \sum_{k=0}^{K}\left(WTD_k \cdot \sum_{h=0}^{H}\left(P_{IMP,h,k}\cdot c_{buy,el} - P_{EXP,h,k}\cdot c_{sell,el}\right)\right) \tag{2}$$

So the objective function is defined as:

$$f(x) = min(Cost_{yearly}) = min(Cost_{INV} + Cost_{OP}) \tag{3}$$

2.2.3 Constraints

This section presents a comprehensive list of all constraints employed to formulate the model.
In certain constraints, a variable M is utilized, where M denotes a sufficiently large number employed to formulate a set of binary constraints (in this work, M is set to 1000).

PV:

$$P_{PV,h,k} = \frac{Cap_{PV}\cdot SolRad_{h,k}}{1000} \qquad for \quad h = 0,\ 1, ..., H, \quad for \quad k = 0,\ 1, ..., K \tag{4}$$

This constraint links the capacity with power output of the PV.

HP:

$$\theta_{HP,h,k,i} \leq \delta_{HP,h,k,i}\cdot M \tag{5}$$

$$Cap_{HP,i} - \theta_{HP,h,k,i} \leq (1-\delta_{HP,h,k,i})\cdot M \tag{6}$$

$$Cap_{HP,i} - \theta_{HP,h,k,i} \geq (1-\delta_{HP,h,k,i})\cdot 0 \tag{7}$$

$$Q_{HP,h,k,i} \leq \theta_{HP,h,k,i} \tag{8}$$

$$Q_{HP,h,k,i} \geq minload_{HP} \cdot Cap_{HP,i} \cdot \delta_{HP,h,k,i} \tag{9}$$

$$P_{HP,h,k,i} = \frac{Q_{HP,h,k,i} \cdot LinCoef_{var} + \delta_{HP,h,k,i} \cdot LinCoef_{fix}}{COP_{ID,h,k}} \tag{10}$$

$$where: \quad COP_{ID,h,k} = \frac{1}{1 - \frac{T_{amb,h,k}}{T_{supply,HP}}} \tag{11}$$

For every equation the constraint is applied $for\ \ h = 0,\ 1, ..., H, \quad for\ \ k = 0,\ 1, ..., K, \quad for\ \ i = 0,\ 1, ..., P$
Using a binary constraint the heat output is constrained between a minimum and a maximum and then the heat output is linked to power consumption through the COP and a linearization.

AC:

$$\theta_{AC,h,k,i} \leq \delta_{AC,h,k,i} \cdot M \tag{12}$$

$$Cap_{AC,i} - \theta_{AC,h,k,i} \leq (1 - \delta_{AC,h,k,i}) \cdot M \tag{13}$$

$$Cap_{AC,i} - \theta_{AC,h,k,i} \geq (1 - \delta_{AC,h,k,i}) \cdot 0 \tag{14}$$

$$C_{AC,h,k,i} \leq \theta_{AC,h,k,i} \tag{15}$$

$$C_{AC,h,k,i} \geq minload_{AC} \cdot Cap_{AC,i} \cdot \delta_{AC,h,k,i} \tag{16}$$

$$P_{AC,h,k,i} = \frac{C_{AC,h,k,i} \cdot LinCoef_{var} + \delta_{AC,h,k,i} \cdot LinCoef_{fix}}{EER_{ID,h,k}} \tag{17}$$

$$where: \quad EER_{ID,h,k} = \frac{1}{\frac{T_{amb,h,k}}{T_{supply,AC}} - 1} \tag{18}$$

For every equation the constraint is applied $for\ \ h = 0,\ 1, ..., H, \quad for\ \ k = 2 \quad for\ \ i = 0,\ 1, ..., P$
Using a binary constraint the cold output is constrained between a minimum and a maximum and then the cold output is linked to power consumption through the EER and a linearization.

EES:

$$SOC_{EES,h+1,k} = SOC_{EES,h,k} \cdot (1 - sd_{EES}) + P_{c,EES,h,k} \cdot \sqrt{\eta_{rt,EES}} - P_{d,EES,h,k} \cdot \sqrt{\eta_{rt,EES}} \tag{19}$$

$$\theta_{c,EES,h,k} \leq \delta_{EES,h,k} \cdot M \tag{20}$$

$$Cap_{EES} - \theta_{c,EES,h,k} \leq (1 - \delta_{EES,h,k}) \cdot M \tag{21}$$

$$Cap_{EES} - \theta_{c,EES,h,k} \geq (1 - \delta_{EES,h,k}) \cdot 0 \tag{22}$$

$$\theta_{d,EES,h,k} \leq \delta_{EES,h,k} \cdot M \tag{23}$$

$$Cap_{EES} - \theta_{d,EES,h,k} \leq (1 - \delta_{EES,h,k}) \cdot M \tag{24}$$

$$Cap_{EES} - \theta_{d,EES,h,k} \geq (1 - \delta_{EES,h,k}) \cdot 0 \tag{25}$$

$$P_{c,EES,h,k} \leq c_{inp,EES} \cdot Cap_{EES} \cdot \delta_{EES,h,k} \tag{26}$$

$$P_{d,EES,h,k} \leq c_{out,EES} \cdot Cap_{EES} \cdot (1 - \delta_{EES,h,k}) \tag{27}$$

For every equation the constraint is applied $for\ \ h = 0,\ 1, ..., H, \quad for\ \ k = 0,\ 1, ..., K$

$$SOC_{EES,h,k} \leq Cap_{EES} \qquad for\ \ h = 0,\ 1, ..., H+1, \quad for\ \ k = 0,\ 1, ..., K \tag{28}$$

$$SOC_{EES,0,k} = SOC_{EES,H,k} \qquad for\ \ k = 0,\ 1, ..., K \tag{29}$$

First, the state of charge is temporally linked. Next, using two sets of binary constraints the charge and discharge power are constrained between a minimum and a maximum. At the end, the SOC is limited to the capacity of the storage and the SOC is linked temporally between subsequent days.

TES:

$$SOC_{TES,h+1,k,i} = SOC_{TES,h,k,i} \cdot (1 - sd_{TES}) + P_{c,TES,h,k,i} \cdot \sqrt{\eta_{rt,TES}} - P_{d,TES,h,k,i} \cdot \sqrt{\eta_{rt,TES}} \tag{30}$$

$$\theta_{c,TES,h,k,i} \leq \delta_{TES,h,k,i} \cdot M \tag{31}$$

$$Cap_{TES,i} - \theta_{c,TES,h,k,i} \leq (1 - \delta_{TES,h,k,i}) \cdot M \tag{32}$$

$$Cap_{TES,i} - \theta_{c,TES,h,k,i} \geq (1 - \delta_{TES,h,k,i}) \cdot 0 \tag{33}$$

$$\theta_{d,TES,h,k,i} \leq \delta_{TES,h,k,i} \cdot M \tag{34}$$

$$Cap_{TES,i} - \theta_{d,TES,h,k,i} \leq (1 - \delta_{TES,h,k,i}) \cdot M \tag{35}$$

$$Cap_{TES,i} - \theta_{d,TES,h,k,i} \geq (1 - \delta_{TES,h,k,i}) \cdot 0 \tag{36}$$

$$P_{c,TES,h,k,i} \leq c_{inp,TES} \cdot Cap_{TES,i} \cdot \delta_{TES,h,k,i} \tag{37}$$

$$P_{d,TES,h,k,i} \leq c_{out,TES} \cdot Cap_{TES,i} \cdot (1 - \delta_{TES,h,k,i}) \tag{38}$$

For every equation the constraint is applied $for\ \ h = 0,\ 1, ..., H, \quad for\ \ k = 0,\ 1, ..., K, \quad for\ \ i = 0,\ 1, ..., P$

$$SOC_{TES,h,k,i} \leq Cap_{TES,i} \qquad for\ \ h = 0,\ 1, ..., H+1, \quad for\ \ k = 0,\ 1, ..., K, \quad for\ \ i = 0,\ 1, ..., P \tag{39}$$

$$SOC_{TES,0,k,i} = SOC_{TES,H,k,i} \qquad for\ \ k = 0,\ 1, ..., K, \quad for\ \ i = 0,\ 1, ..., P \tag{40}$$

First, the state of charge is temporally linked. Next, using two sets of binary constraints the charge and discharge power are constrained between a minimum and a maximum. At the end, the SOC is limited to the capacity of the storage and the SOC is linked temporally between subsequent days.

House electricity load:

$$\sum_{h=0}^{H} \delta_{wash,h,k,i} = qt_{wash} \tag{41}$$

$$P_{wash,h,k,i} = \delta_{wash,h,k,i} \cdot RP_{wash} \tag{42}$$

For every equation the constraint is applied $for\ \ h = 0,\ 1, ..., H, \quad for\ \ k = 0,\ 1, ..., K, \quad for\ \ i = 0,\ 1, ..., P$

$$P_{wash,h+1,k,i} = \delta_{wash,h,k,i} \cdot RP_{wash} \quad for\ \ h = 0,\ 1, ..., H+1, \quad for\ \ k = 0,\ 1, ..., K, \quad for\ \ i = 0,\ 1, ..., P \tag{43}$$

$$P_{wash,0,k,i} = P_{wash,H,k,i} \qquad for\ \ k = 0,\ 1, ..., K, \quad for\ \ i = 0,\ 1, ..., P \tag{44}$$

$$\sum_{h=0}^{H} \delta_{dish,h,k,i} = qt_{dish} \tag{45}$$

$$P_{dish,h,k,i} = \delta_{dish,h,k,i} \cdot RP_{dish} \tag{46}$$

$$\sum_{h=0}^{H} \delta_{drye,h,k,i} = qt_{drye} \tag{47}$$

$$P_{drye,h,k,i} = \delta_{drye,h,k,i} \cdot RP_{drye} \tag{48}$$

$$Dem_{El,h,k} = Dem_{El,base,h,k} \cdot P + \sum_{i=0}^{P} (P_{wash,h,k,i} + P_{dish,h,k,i} + P_{drye,h,k,i}) \tag{49}$$

For every equation the constraint is applied $for\ \ h = 0,\ 1, ..., H, \quad for\ \ k = 0,\ 1, ..., K, \quad for\ \ i = 0,\ 1, ..., P$

First, the number of activations is linked to the number of the appliances. Next, the temporal slot is assigned using the binary variable. This is done for each type of appliance. At the end all the appliances consumption are summed to the base consumption to generate the electrical demand.

House heating load:

$$Q_{DHW,hourly} = \frac{\rho_w \cdot c_{p,w} \cdot V_{DHW,day} \cdot (T_{out} - T_{in})}{24} \tag{50}$$

This constraint is used to calculate the heating demand for DHW in the case it was evenly spread across the 24 hours.

$$Q_{DHW,h,k} = c_{usage,h,k} \cdot Q_{DHW,hourly} \tag{51}$$

Instead, in this constraint the heating demand for DHW is distributed at given hours as units of hour equivalent consumptions. Following is a table showing the distribution:

h	c_{usage}
7	1
8	10
18	2
19	8
20	2
21	1

Table 10: Distribution of DHW usage during the day

$$R_{wall} = \sum_{j} \frac{d_j}{\lambda_j \cdot A} \tag{52}$$

$$R_{air,amb} = \frac{1}{\frac{n}{3600} \cdot V_{air} \cdot \rho_{air} \cdot c_{p,air}} \tag{53}$$

$$C_{wall} = \sum_{j} \rho_j \cdot c_{p,j} \cdot d_j \cdot A \tag{54}$$

$$C_{air} = \sum_{j} \rho_j \cdot c_{p,j} \cdot V_{air} \tag{55}$$

These constraints are employed to construct the heat dispersion model, utilizing the electrical circuit equivalent. The circuit is configured as follows:

- The resistance of the wall is split into two identical halves.
- The heating is subdivided into two heat sources, one flowing to the air and the other to the wall.
- Another heat source is the heat absorbed by the air from the solar radiation.
- The lower branch represents dispersions of heat through the wall, while the upper branch represents dispersions through ventilation.
- On the lower branch the external temperature considers a surface temperature of the wall, by taking into account the absorption of solar radiation and the convection dispersion.

This model is constructed starting from [27], adapting it to a simpler circuit (2R1C with an added resistance and capacitance).

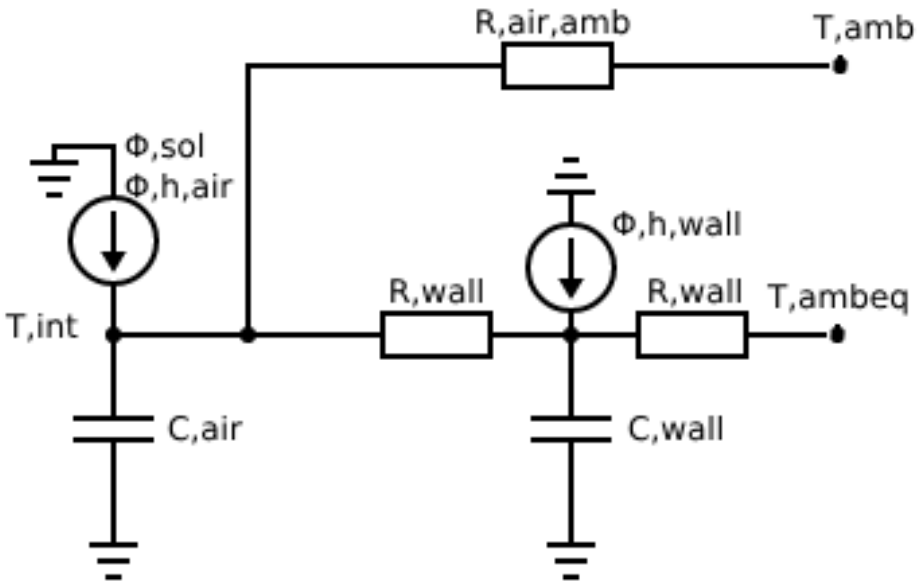

Figure 1: Winter circuit equivalent

The summer circuit differs only in that the cold source exclusively flows through the internal air.

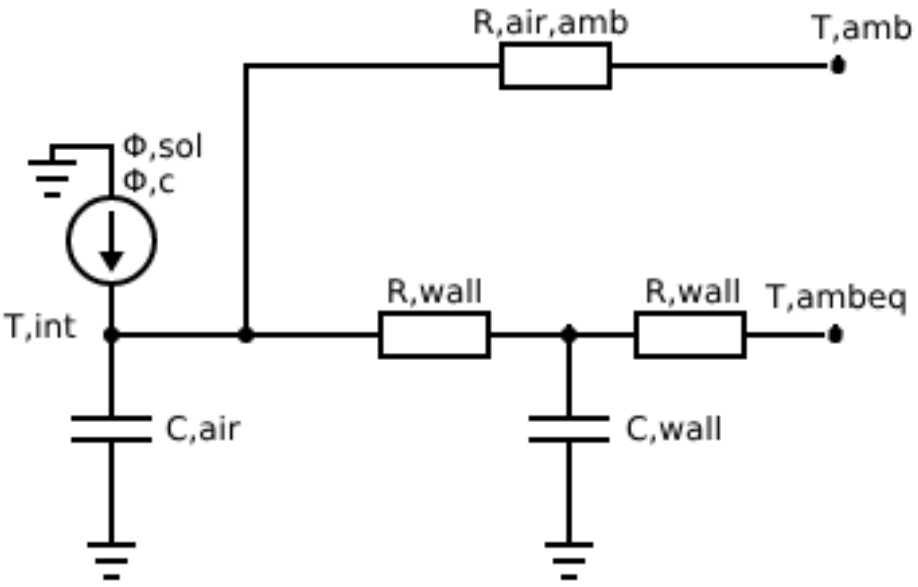

Figure 2: Summer circuit equivalent

$$\Phi_{h,air,h,k,i} = (1 - f_{heat,rad}) \cdot \Phi_{h,h,k,i} \tag{56}$$

$$\Phi_{h,wall,h,k,i} = f_{heat,rad} \cdot \Phi_{h,h,k,i} \tag{57}$$

$$\Phi_{sol,h,k} = f_{sol} \cdot SolRad_{h,k} \tag{58}$$

$$T_{amb,eq,h,k} = T_{amb,h,k} + SolRad_{h,k} \cdot \frac{h_f}{h_A} \tag{59}$$

For every equation the constraint is applied $for \;\; h = 0,\; 1, ..., H, \quad for \;\; k = 0,\; 1, ..., K$

$$C_{air,h,k,i} \cdot (T_{int} - T_{int,h-1,k,i}) = \frac{T_{wall,h,k,i} - T_{int,h,k,i}}{R_{wall}} + \frac{T_{amb,h,k,i} - T_{int,h,k,i}}{R_{air,amb}} + \Phi_{sol,h,k} + \Phi_{h,air,h,k,i} \tag{60}$$

$$C_{wall,h,k,i} \cdot (T_{wall,h,k,i} - T_{wall,h-1,k,i}) = \frac{T_{int,h,k,i} - T_{wall,h,k,i}}{R_{wall}} + \frac{T_{amb,eq,h,k,i} - T_{wall,h,k,i}}{R_{wall}} + \Phi_{h,wall,h,k,i} \tag{61}$$

For every equation the constraint is applied $for \;\; h = 0,\; 1, ..., H, \quad for \;\; k = 0,\; 1,\; 3, \quad for \;\; i = 0,\; 1, ..., P$

$$C_{air,h,k,i} \cdot (T_{int} - T_{int,h-1,k,i}) = \frac{T_{wall,h,k,i} - T_{int,h,k,i}}{R_{wall}} + \frac{T_{amb,h,k,i} - T_{int,h,k,i}}{R_{air,amb}} + \Phi_{sol,h,k} - \Phi_{c,h,k,i} \tag{62}$$

$$C_{wall,h,k,i} \cdot (T_{wall,h,k,i} - T_{wall,h-1,k,i}) = \frac{T_{int,h,k,i} - T_{wall,h,k,i}}{R_{wall}} + \frac{T_{amb,eq,h,k,i} - T_{wall,h,k,i}}{R_{wall}} \tag{63}$$

For every equation the constraint is applied $for \;\; h = 0,\; 1, ..., H, \quad for \;\; k = 2, \quad for \;\; i = 0,\; 1, ..., P$

$$Dem_{Th,h,k,i} = Q_{DHW,h,k,i} + \Phi_{h,h,k,i} \tag{64}$$

For every equation the constraint is applied $for \;\; h = 0,\; 1, ..., H, \quad for \;\; k = 0,\; 1, ..., K, \quad for \;\; i = 0,\; 1, ..., P$

This constraint is used to establish the thermal demand equal to the sum of DHW heat demand and the heating demand.

$$T_{int,h,k,i} \geq T_{target,k} - T_{variation} \tag{65}$$

$$T_{int,h,k,i} \leq T_{target,k} + T_{variation} \tag{66}$$

$$T_{int,h+1,k,i} \geq T_{int,h,k,i} - 2.2 \tag{67}$$

$$T_{int,h+1,k,i} \leq T_{int,h,k,i} + 2.2 \tag{68}$$

For every equation the constraint is applied $for\ \ h = 0,\ 1, ..., H, \quad for\ \ k = 0,\ 1, ..., K, \quad for\ \ i = 0,\ 1, ..., P$

$$T_{int,h,k,i} \geq T_{amb,h,k} \tag{69}$$

For every equation the constraint is applied $for\ \ h = 0,\ 1, ..., H, \quad for\ \ k = 0,\ 1,\ 3, \quad for\ \ i = 0,\ 1, ..., P$

In this last section the first two constraints set a maximum boundary for the internal temperature. The second two are used to set the maximum change in internal temperature, following ASHRAE guidelines [28] (Table 5.3.4.3). The last constraint is used to set the internal temperature to be at least as high as the ambient temperature in all seasons except summer.

Electrical energy balance:

$$-Dem_{El,h,k} + P_{imp,h,k} - P_{exp,h,k} + P_{PV,h,k} - \sum_{i=0}^{P}(P_{HP,h,k,i} + P_{AC,h,k,i}) + P_{d,EES,h,k} - P_{c,EES,h,k} = 0 \tag{70}$$

For every equation the constraint is applied $for\ \ h = 0,\ 1, ..., H, \quad for\ \ k = 0,\ 1, ..., K, \quad for\ \ i = 0,\ 1, ..., P$

This constraint is used to set the sum of consumptions and productions of electricity to zero.

Thermal energy balance:

$$-Dem_{Th,h,k,i} + Q_{HP,h,k,i} + Q_{d,TES,h,k,i} - Q_{c,TES,h,k,i} = 0 \tag{71}$$

For every equation the constraint is applied $for\ \ h = 0,\ 1, ..., H, \quad for\ \ k = 0,\ 1, ..., K, \quad for\ \ i = 0,\ 1, ..., P$

The first constraint is used to set the sum of consumptions and productions of heat to zero and the second constraint is used to set the sum of consumptions and productions of cold to zero.

$$-\Phi_{c,h,k,i} + C_{AC,h,k,i} = 0 \tag{72}$$

For every equation the constraint is applied $for\ \ h = 0,\ 1, ..., H, \quad for\ \ k = 2, \quad for\ \ i = 0,\ 1, ..., P$

House comfort:

Electrical comfort:

$$\sum_{h=0}^{H}(\delta_{wash,h,k,i} \cdot (h - trg_{wash,i})^2 + \delta_{dish,h,k,i} \cdot (h - trg_{dish,i})^2 + \delta_{drye,h,k,i} \cdot (h - trg_{drye,i})^2) \leq trg_{ElCom,i} \tag{73}$$

The electrical comfort is constructed starting from the difference for each appliance between the target start time of the appliance and the real start time. This difference is then squared to both accentuate the loss of comfort as the start time deviates further from the target start time and to have in all cases a positive result from the difference. The activation variable allows to pick the right time slot for the calculation of this difference. The differences for each appliance are then summed and are set to be lower or equal than a given threshold.
Thermal comfort:

$$\sum_{h=0}^{H}((T_{int,h,k,i} - T_{target,k})^2 \cdot occ_k) \leq trg_{ThCom,i} \tag{74}$$

For every equation the constraint is applied $for\ \ h = 0,\ 1, ..., H, \quad for\ \ k = 0,\ 1, ..., K, \quad for\ \ i = 0,\ 1, ..., P$
The thermal comfort is constructed starting from the difference for each hour between the target temperature and the real internal temperature. This difference is then squared to both accentuate the loss of comfort as the internal temperature deviates further from the target and to have in all cases a positive result from the difference. The differences for each hour are then summed for the whole day and are set to be lower or equal than a given threshold.

2.3 Demand Side Management strategies

In this section, three types of DSM strategies are detailed. First two basic types of DR are introduced, the PBDR and the IBDR, included to establish an initial comparison for the optimizer DR. Unlike for the optimizer DR, constraints 41 through 49 were not implemented for these two DR types. Instead, specific constraints detailed in the subsequent paragraphs were employed to execute the DR. The constraints and values for these models were derived from [12].

2.3.1 Price Based DR

Price-Based Demand Response (PBDR) typically relies on a Time of Use (ToU) electricity tariff to induce a response in user consumption. High electricity prices, often corresponding to peak periods in the electrical network, act as a deterrent for consumption among participating users.
The implemented ToU tariff is presented in the following table.

Time slot	Electricity price $[\frac{c€}{kWh}]$
0:00 - 4:00	6
5:00 - 9:00	31
10:00 - 17:00	6
18:00 - 19:00	31
20:00 - 22:00	19
23:00 - 0:00	6

Table 11: ToU electricity tariff

The following constraints are employed to allow a variation in the electricity demand:

$$P_{el,h,k,DR} \leq P_{el,h,k} \cdot (1 + d_L) \tag{75}$$

$$P_{el,h,k,DR} \geq P_{el,h,k} \cdot (1 - d_L) \tag{76}$$

$$P_{el,h,k,DR} \leq max(P_{el,h,k}) \tag{77}$$

$$P_{el,h,k,DR} \geq min(P_{el,h,k}) \tag{78}$$

$$\sum_{h=0}^{23} E_{el,h,k,DR} = \sum_{h=0}^{23} E_{el,h,k} \tag{79}$$

For every equation the constraint is applied $for \;\; h = 0,\; 1, ..., H, \quad for \;\; k = 0,\; 1, ..., K$
The value of d_L is selected as 0.2, as derived by [12].

2.3.2 Incentive Based DR

In the Incentive Based DR (IBDR) the driving force of the change in electricity demand is an incentive assigned to the remaining energy after a reduction. The constraints utilized are constraints 75, 76, 77, 78 and three additional constraints:

$$\sum_{h=0}^{23} E_{el,h,k,DR} = d_D \cdot \sum_{h=0}^{23} E_{el,h,k} \tag{80}$$

The incentive is applied only when the consumer reduces its consumption by 5% in respect to its original consumption.

$$\frac{P_{el,h,k} - P_{el,h,k,DR}}{P_{el,h,k}} \geq 0.05 \tag{81}$$

And the revenue is calculated as follows:

$$rev_{IBDR,k} = \sum_{h=0}^{23} (E_{el,h,k} - E_{el,h,k,DR}) \cdot inc_{IBDR} \tag{82}$$

For every equation the constraint is applied $for \;\; h = 0,\; 1, ..., H, \quad for \;\; k = 0,\; 1, ..., K$
The electricity price is set to a fixed $19 \frac{c€}{kWh}$ and the incentive is set to $8 \frac{c€}{kWh}$. The value of d_D is used to introduce the possibility of a reduction of the overall energy consumed during a day.

2.3.3 Optimizer DR

This type of DR entails providing the optimizer with the possibility to shift two types of load: Shiftable Appliances (SAs) and Controllable Appliances (CAs).
SAs are loads that can be scheduled with no time constrictions, in this work three SAs are considered: a washing machine, a dish washer and a dryer. Their characteristics are listed in Table 7.
On the other hand, CAs are loads that can be only varied between a minimum and a maximum power, in this work there are two: the HP and the AC.
The remainder of the load is categorized as Non-Shiftable Appliances (NSAs), which are loads that must be satisfied within their designated time period, and as such do not concur to the DR.
To give the optimizer a direction for the load shifting the ToU tariffs (given in Table 11),

also applied in the PBDR, is implemented. To limit the variation of load of SAs and CAs, two types of comfort are defined, each related to one type of appliance. The first is the comfort of SAs, defined in this work as "electrical comfort" and expressed in Equation 73. The second pertains to CAs, defined as "thermal comfort" and expressed in Equation 74. Both comforts must be lower than a set limit that defines the desired level of comfort for the user. A higher number indicates lower comfort, as it provides the optimizer with more flexibility to deviate from the standard.

2.4 Analyses

The analyses carried out were designed to achieve the goals established in subsection 1.5. The same base model was employed in all analyses, with specific additions for each case. The primary outcome of an analysis, and the tool used to compare different models and users, is the final unitary price paid. This is calculated in two forms, the first considers only the electrical energy used, while the second also considers the thermal energy. The equations used for calculation are the following:

$$COE_e = \frac{Cost_{INV} + Cost_{OP}}{\sum_{k=0}^{K}(WTD_k \cdot \sum_{h=0}^{H}(Dem_{El,h,k} \cdot P))} \tag{83}$$

$$COE_t = \frac{Cost_{INV} + Cost_{OP}}{\sum_{k=0}^{K}(WTD_k \cdot \sum_{h=0}^{H}(Dem_{El,h,k} \cdot P + \sum_{i=0}^{P}(P_{HP,h,k,i} + P_{AC,h,k,i})))} \tag{84}$$

This approach provides a metric for the Cost of Energy (COE) for both an individual user and an EC.
When analyzing an EC, for simplicity, it is assumed that thermal generation and storage are not shared and are instead individually determined and controlled. This assumption is made to avoid complications associated with the sharing of thermal energy within an EC, that would require a shared heating network. Conversely, electricity generation and storage are designed and optimized for the EC as a single user.

2.4.1 Preliminary analysis - DR techniques comparison

Before delving into a detailed analysis of the optimizer DR, it is prudent to assess whether this DR technique outperforms the two basic DSM strategies outlined in subsubsection 2.3.1 and in subsubsection 2.3.2. To ensure a fair comparison, the thermal aspect was not integrated, and a fixed thermal load is imposed on all three DR models. This allows for a comparison solely in the electrical side, while the integration of the thermal-side DR management would most likely introduce additional savings for the optimizer DR. For this analysis, no limit on electrical comfort is set, to appreciate the maximum achievable savings.
To provide baseline comparisons, two base case scenarios are introduced. In the first scenario, all the electricity is bought from the grid at $8\frac{c€}{kWh}$ and the thermal demand is met with a boiler with $\eta = 0.97$ and a natural gas cost of $98\frac{€}{MWh}$. The second scenario represents an optimized case, where the model provides an optimal design and operation without any DR.

2.4.2 Analysis of a single house

To achieve and validate goal number two *"Implement DSM strategies for the residential users, enabling the shifting of loads and characterize the loss of electrical and thermal comfort of the user."* a simulation of a single house is carried out. The electrical and thermal comforts levels are set respectively at a threshold of 6 and 20. The electric and thermal energy balance are analyzed, along with the comfort component for each day, to validate the logic behind the optimizer's decisions. Lastly the capacities of the installed generators and storages are evaluated and a COE is provided as a reference for future analyses. Another insightful metric for the single household is the ratio of produced electricity that is self-consumed to the consumed electricity, defined as:

$$SC_{el} = 1 - \frac{\sum_{k=0}^{K} \sum_{h=0}^{H} P_{imp,h,k}}{\sum_{k=0}^{K} \sum_{h=0}^{H} Dem_{El,h,k} \cdot P + \sum_{i=0}^{P} (P_{HP,h,k,i} + P_{AC,h,k,i})} \tag{85}$$

and the ratio of sold electricity to the generated electricity, defined as:

$$SO_{el} = \frac{\sum_{k=0}^{K} \sum_{h=0}^{H} P_{exp,h,k}}{\sum_{k=0}^{K} \sum_{h=0}^{H} P_{PV,h,k}} \tag{86}$$

2.4.3 Analysis of the comfort-savings trend

To achieve the third goal, which is *"Quantify the savings generated from the implementation of DSM and verify the correlation between savings and loss of comfort of the user."* the best course of action, starts with conducting an iterative analysis on a single household. This aims to discern any trend in the correlation between comfort and savings. For this purpose, COE-comfort graphs are generated, offering a detailed view on the trend in comfort-savings correlation.

2.4.4 Analysis of an EC composed of single houses

As stated in goal number four *"Evaluate the performance of the model when integrated within an EC."* an EC is analyzed. In this first EC analysis, the participants are all single households with load shifting. The analysis is carried out as a parametric analysis, with the number of houses participating in the EC being the varied parameter. The analyzed scenario tests if the collaboration of houses could further improve the economic advantage of the single users. For example, the collaboration of households with load shifting could achieve savings by reducing the installed capacities by moving all the loads to a better suited time slot. Or inversely, could decide to focus the appliances during the day to better exploit the PV generation. To test this, a simulation is performed on an EC composed of the same single household, adding one household at a time to evaluate the COE for the EC.
The size of the analysis is kept small, as the simulation time grows rapidly due to the combinatory nature of the scheduling decisions the optimizer has to make.

2.4.5 Analysis of an EC composed of residential users with and without load shifting

To further develop the fourth goal another analysis is performed. This analysis aims to ascertain whether a user employing load shifting can yield additional savings when integrated into an EC alongside households without load shifting capabilities. The analysis is carried out by first fixing number of load-shifting-capable users, and then by varying the number of ordinary residential users. The loads of the ordinary residential Specifically, their thermal load is individually met through a combination of a HP and TES. Conversely, the electrical load is assigned to the entire community, consistent with the approach adopted in the previous analysis.

2.4.6 Analysis of an EC composed of residential users and an industrial user

To further diversify the types of ECs analyzed, and thus better fulfill the objectives outlined in goal number four, an additional analysis is conducted. In this analysis, users employing load shifting are aggregated within an EC alongside an industrial user characterized by a fixed electrical and thermal load, with an overall load higher than those of the residential users. The number of residential users is varied to observe if potential trends emerge. The purpose of this analysis is to determine whether variations in the magnitude and shape of the demand curve influence the behavior of a load-shifting user and, if so, in what manner and to identify potential savings. The comforts level of the load shifting users are set to 6 for electrical and 20 for thermal comfort.

2.4.7 Analysis of an EC composed of an industrial user and residential users with and without load shifting

As a final analysis on ECs and to complete the overview to reach the fourth goal, one final analysis is carried out. In this analysis a combination of the two previous analyses is performed, incorporating an industrial user alongside a diverse group of residential users, some equipped with load-shifting capabilities and others without. The objective is to evaluate whether such a combination of user types within an EC can yield economic advantages.

2.4.8 Sensitivity analyses

Lastly, a series of sensitivity analyses are carried out to assess the influence of certain variables on the system's outcomes. The model tested is the single household analyzed in subsubsection 2.4.2, this model is chosen for its simplicity and significance in relation to all the models examined. Only one variable is analyzed at the time, while the others remain the same. Below is a list of all analyzed variables, along with their respective variations.

Variable	Unit	Variations			
$cbuy_{el}$	$[\frac{c€}{kWh}]$	+25%	+50%	+100%	+200%
$cbuy_{el}$ and $csell_{el}$	$[\frac{c€}{kWh}]$	-50%	-25%	+25%	+50%
Investment costs	[€]	-20%	-10%	+25%	+50%
Interest rate r	-	2%	4%	6%	8%
$f_{heat,rad}$	-	50%	65%	85%	95%
f_{sol}	-	-50%	-25%	+25%	+50%
h_f	-	-50%	-25%	+25%	+50%
h_A	-	-30%	-15%	+25%	+50%
V_{house}	$[m^3]$	-50%	-25%	+100%	+200%
n_{air}	$[h^{-1}]$	-50%	-25%	+25%	+50%
V_{DHW}	$[\frac{m^3}{day}]$	-50%	-25%	+25%	+50%
d_{wall}	$[m]$	-50%	-25%	+25%	+50%
λ_{wall}	$[\frac{W}{m^2 \cdot K}]$	-50%	-25%	+25%	+50%
ρ_{wall}	$[\frac{kg}{m^3}]$	-50%	-25%	+25%	+50%
$c_{p,wall}$	$[\frac{J}{kg \cdot K}]$	-50%	-25%	+25%	+50%
T_{target}	[°C]	18/28	19/27	22/24	26/20
T_{var}	[°C]	1	2	4	5
time of appliances	$[h]$	-10	-2	2	12
time of DHW	$[h]$	-10	-2	2	12
occupancy	$[h]$	-10	-2	2	12
SolRad	$[\frac{W}{m^2}]$	-50%	-25%	+25%	+50%
T_{amb}	[°C]	-4	-2	4	8

Table 12: Variations in sensitivity analysis

3) Results

The first result presented in this section is that this model is economically advantageous when compared to two basic types of Demand Response, Price Based and Incentive Based. It achieves a 26% reduction in yearly costs compared to a base case, while the Incentive Based and the Price Based respectively achieve a 17% and a 19%.
Subsequently, as the model is proven to perform better, this type of user is aggregated in various configurations of Energy Communities to ascertain if there is a potential for additional savings for the user, as the capability of load shifting could benefit the Energy Community.
For the single residential household the COE amounts to 25.83 $\frac{c€}{kWh}$ for the COE_e and 19.65 $\frac{c€}{kWh}$ for the COE_t. The installed capacities for the single household comprise of 2.28 kWp of PV, 3.13 kWth of HP, 1.02 kWh of TES and 1.41 kWh of EES.
Following this, the model is integrated into an EC. Initially, an analysis is conducted on a community exclusively composed of single households with load shifting. The observed trend indicates is nearly constant, with the COE remaining almost flat. Next, an EC comprising both residential users employing load shifting and residential users who do not, is analyzed. As the number of users without load shifting increases, there is a corresponding increase in the COE, demonstrating a direct correlation. This holds true irrespective of the number of users with load shifting. In the subsequent phase, the introduction of an industrial user takes place. The EC undergoes testing initially with solely load-shifting users, and then with a combination of load-shifting and non-load-shifting users. In both scenarios, the COE is lower than that of individual single households but exceeds the COE of the industrial user operating independently. Consequently, it becomes evident that the model, in its current state, does not present an economically advantageous path for the establishment of an EC.

3.1 DR comparison

As specified in subsubsection 2.4.1, the analysis is performed to estimate if the proposed model would provide an economic advantage over some simpler DR techniques. The hourly maximum variation d_L is set to 0.2, the daily energy reduction for the IBDR d_D is set to 0.05 to give the two basic models more competitiveness over the optimizer model.

	Optimized reference	IBDR	PBDR	Optimizer DR
PV [kWp]	3,1	3,07	3,16	1,56
HP [kWth]	2,15	2,17	2,01	2
TES [kWh]	1,45	1,36	2,21	2,26
EES [kWh]	0	0	1,68	0,9

Table 13: Installed capacities of the preliminary DR technique comparison

	Annual actualized costs $[\frac{€}{yr}]$
Base reference	2293
Optimized reference	1999
IBDR	1903
PBDR	1860
Optimizer DR	1689

Table 14: Annual actualized costs of the preliminary DR technique comparison

Remembering that the base case is set to be where all the electricity is bought from the grid and the heat demand is satisfied by a natural gas boiler the conclusions are the following. Since the energy demand for all the cases is the same the direct costs comparison is fair, and the results shown in the tables highlight that:

- A simple, well-sized design of a household can bring savings (around 13%).
- All the DR techniques tested provide a meaningful amount of savings (the lowest being 17%).
- The best performing DR technique is the optimizer DR with a reduction of around 26% in annual actualized costs.

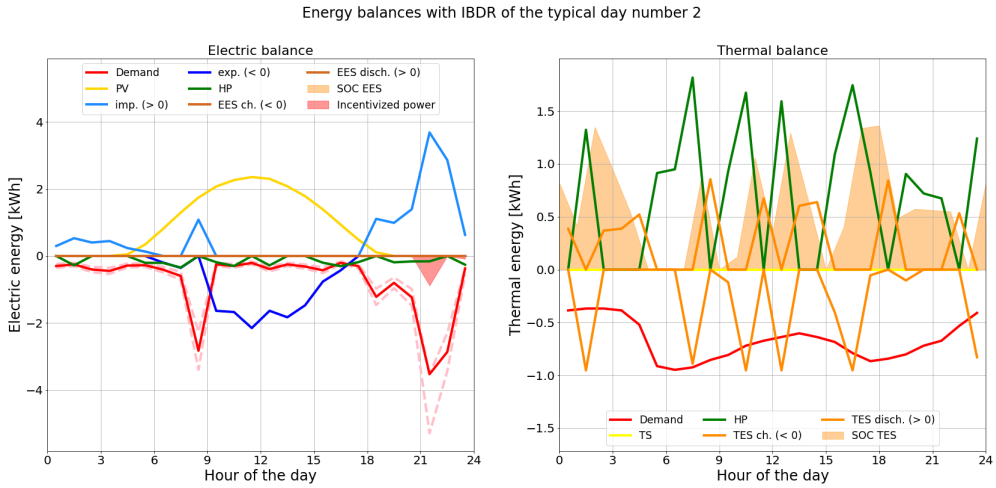

Figure 3: IBDR energy balance for a typical summer day

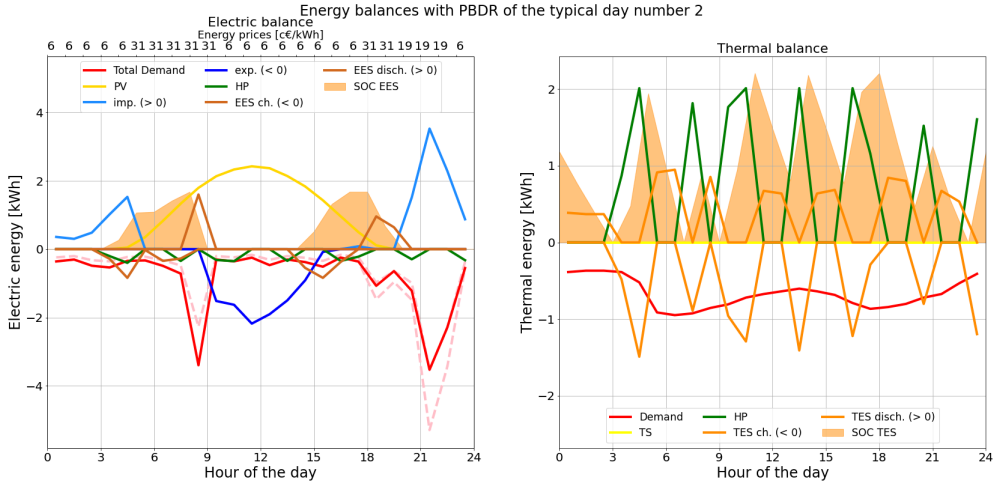

Figure 4: PBDR energy balance for a typical summer day

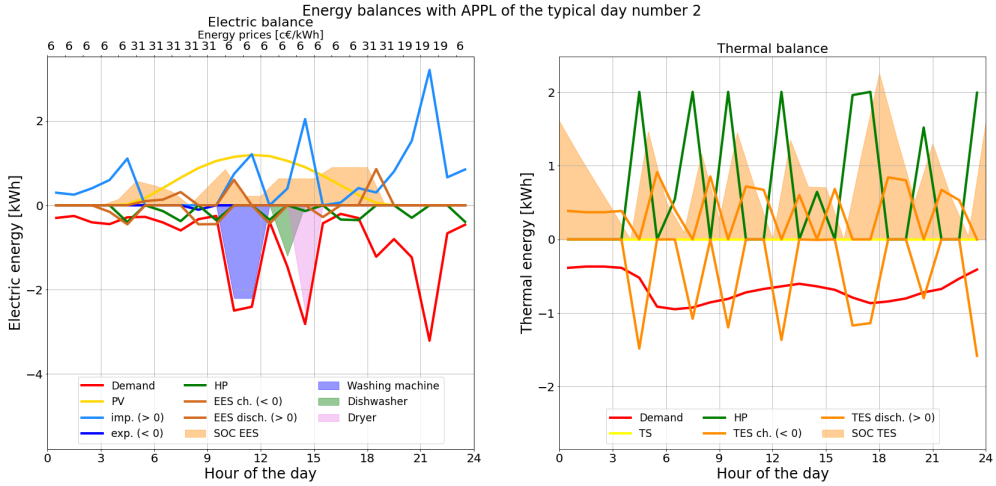

Figure 5: Optimizer DR energy balance for a typical summer day

To breakdown the decisions made by the optimizer and ensure a good logical foundation, let's analyze what is shown in Figure 3 through Figure 5.
Starting from the IBDR, the incentive is actually only received during one hour (21-22). However, the chosen hour is the best possible as, as shown in Equation 82, a higher reduction translates to greater revenue, and the selected hour offers the highest feasible reduction.
For the PBDR it is possible to observe that the optimizer minimizes consumption during time slots 18 through 22, as the electricity price is high and no generation is available. As the total energy during the day needs to be the same, the consumption is maximized during time slots 0 through 16. However, through a combination of the EES, buying during low electricity prices and PV generation, no electricity is bought during high electricity prices, thus leading to greater savings.
In the optimizer DR, a similar principle to the PBDR is applied by the optimizer. However, the majority of peak power consumption is shifted to the middle of the day to capitalize on both PV generation and low electricity prices, thus leading to lower installed capacities of PV and EES.

3.2 Single house analysis

To visualize the choices of the optimizer, two main graphs are employed, one for the electric and thermal balance and another for the electrical and thermal comfort.
In this simulation, the two threshold values for the comfort are set respectively at 6 for the electrical and 20 for the thermal. The reason for these values is explained in subsection 3.3.

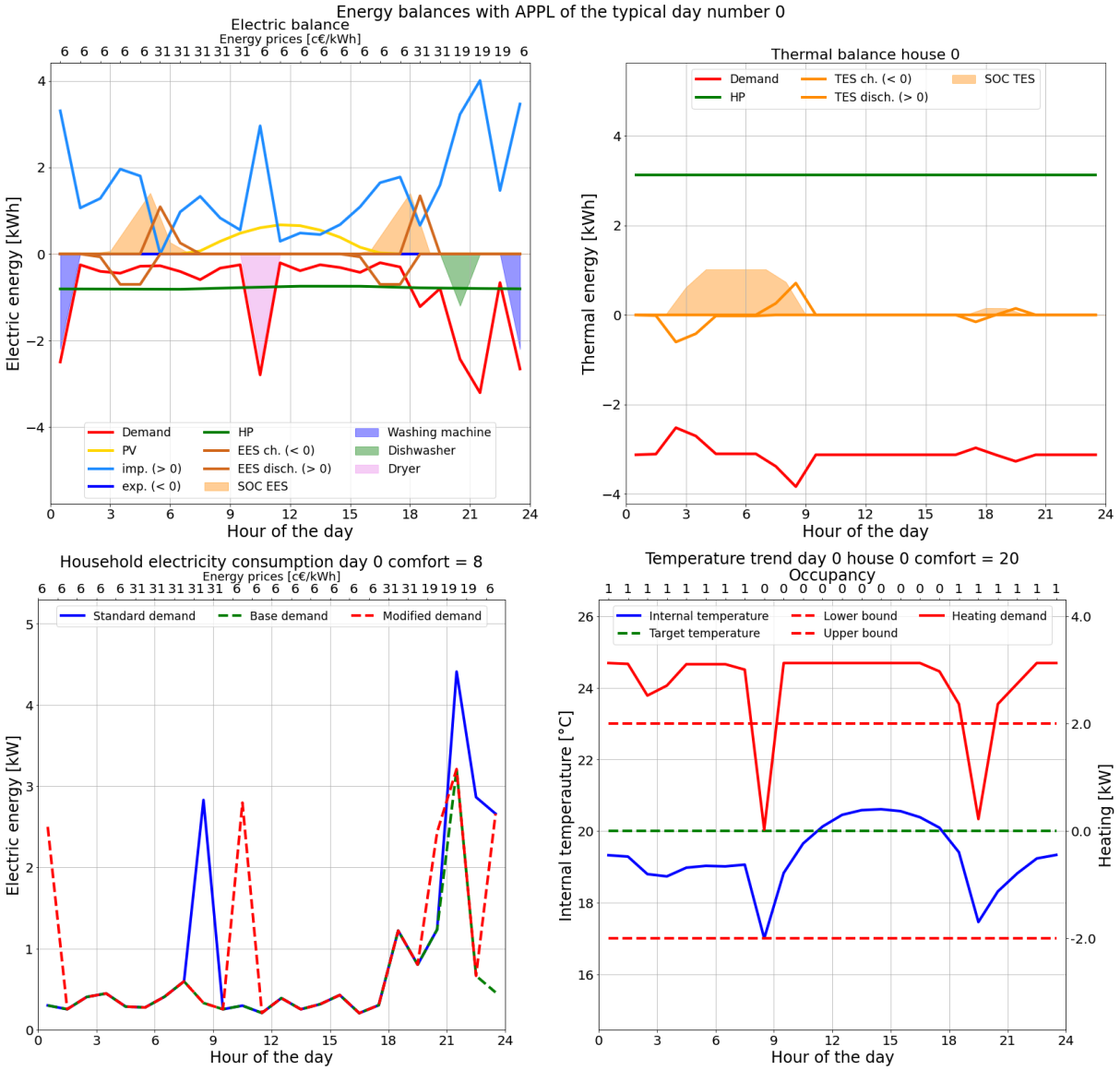

Figure 6: Typical winter day

During the winter day the PV produces very little energy due to low solar radiation, so the main driver in the appliances schedule is the low energy prices. It is possible to notice that the dishwasher is being scheduled for an intermediate price hour (20-21). This scheduling decision is influenced by two factors: prioritization of the other two appliances due to their higher load and, the constraint of electrical comfort, meaning the dishwasher is scheduled during an intermediate price hour. Such compromise is deemed acceptable, as the user's comfort level imposes constraints that may not allow for perfect optimization and such result in lower savings.
In the thermal balance it is possible to observe a near constant load for the heat pump,

exploiting the maximum possible COP. The drops in heating demand are due to the DHW request, and are purposefully timed as to not require a bigger HP size. The first drop in temperature is during a non-occupied hour, so the comfort is not impacted. Another important behaviour that can be observed is that the heating demand is also started during non-occupied hours because the low cost and PV generation, allowing to preheat the house and to have a suitable temperature when occupancy resumes.

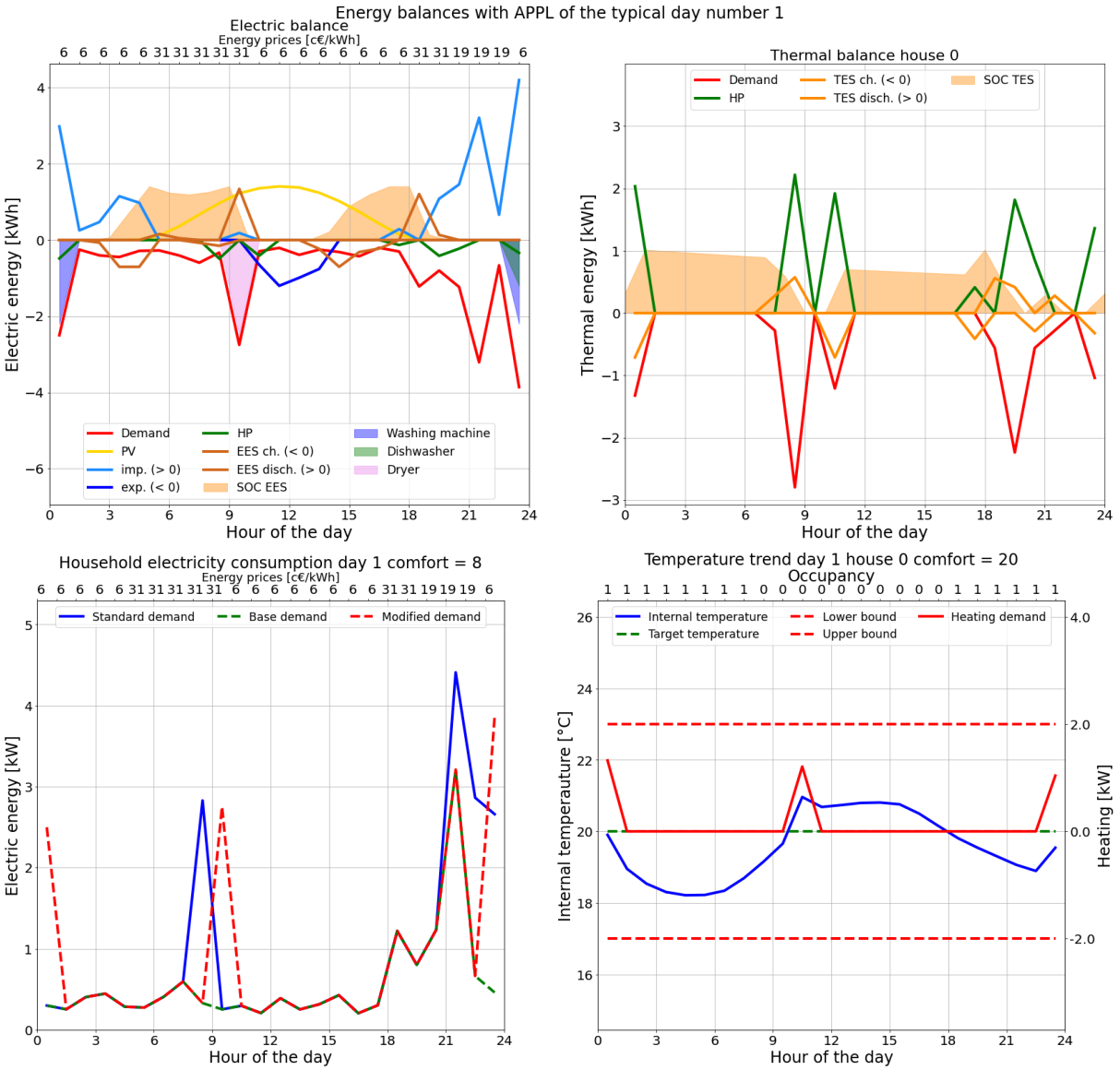

Figure 7: Typical spring day

For the spring day, a pattern emerges, where the EES is used to cover a portion of the load during high electricity price hours. As seen from the graph, during the morning high electricity prices all the electricity comes either from the PV or the EES. Instead, during the evening only the first hour is covered, as the demand is fairly high in the evening hours. For the appliances it is possible to observe that the dryer would be in a high electricity price hour but almost all electricity is supplied by the EES or the PV. This is done to have instead a better placement for the remaining appliances to a low electricity price hour.

For the thermal balance a distinct change in the HP operational mode is observed. The

heating demand is nearly zero, as high enough external temperatures combined with the good insulation of the house are enough to maintain an adequate internal temperature. Consequently, the HP is predominantly employed to provide the DHW, but to produce the thermal demand required the most efficient solution for the HP is to work near maximum capacity, so the TES comes into play, allowing the storage of the excess heat produced by the HP working in this manner. To fulfill the thermal demand efficiently, the HP operates near its maximum capacity as the efficiency is higher, and the TES is utilized to store the excess heat produced when the HP operates at maximum capacity.

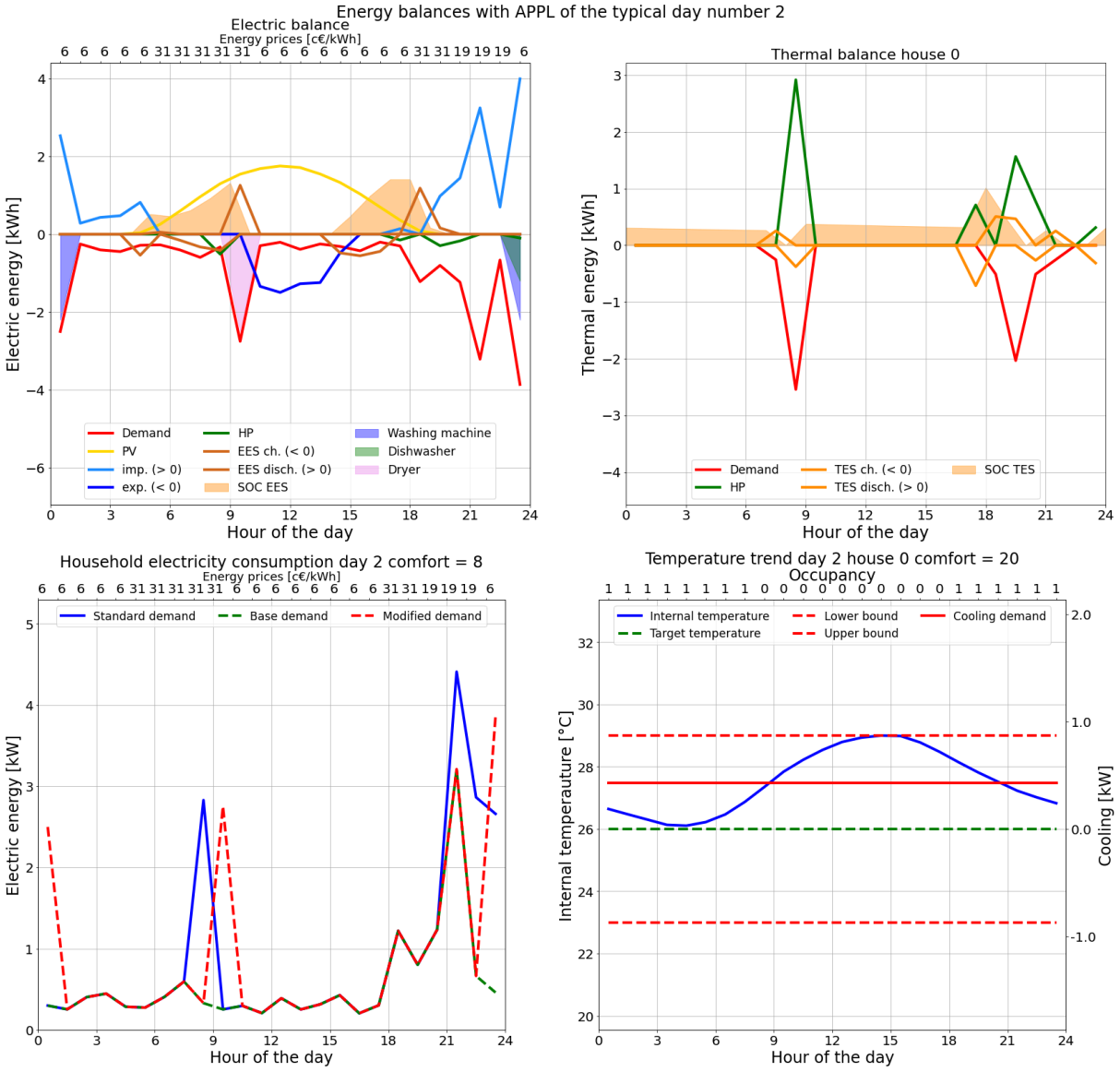

Figure 8: Typical summer day

On the summer day, the PV generation is sufficiently high to cover the demand, charge the EES and even sell some electricity. When the PV stops generating the EES is used to supply some of the electricity required, although most of the electricity is bought from the grid. For everything else the behaviour is the same as the spring day.
For the thermal side, cooling is considered and is applied at a low but constant rate, as the hottest hours are during non-occupied hours and the thermal comfort threshold can still be met.

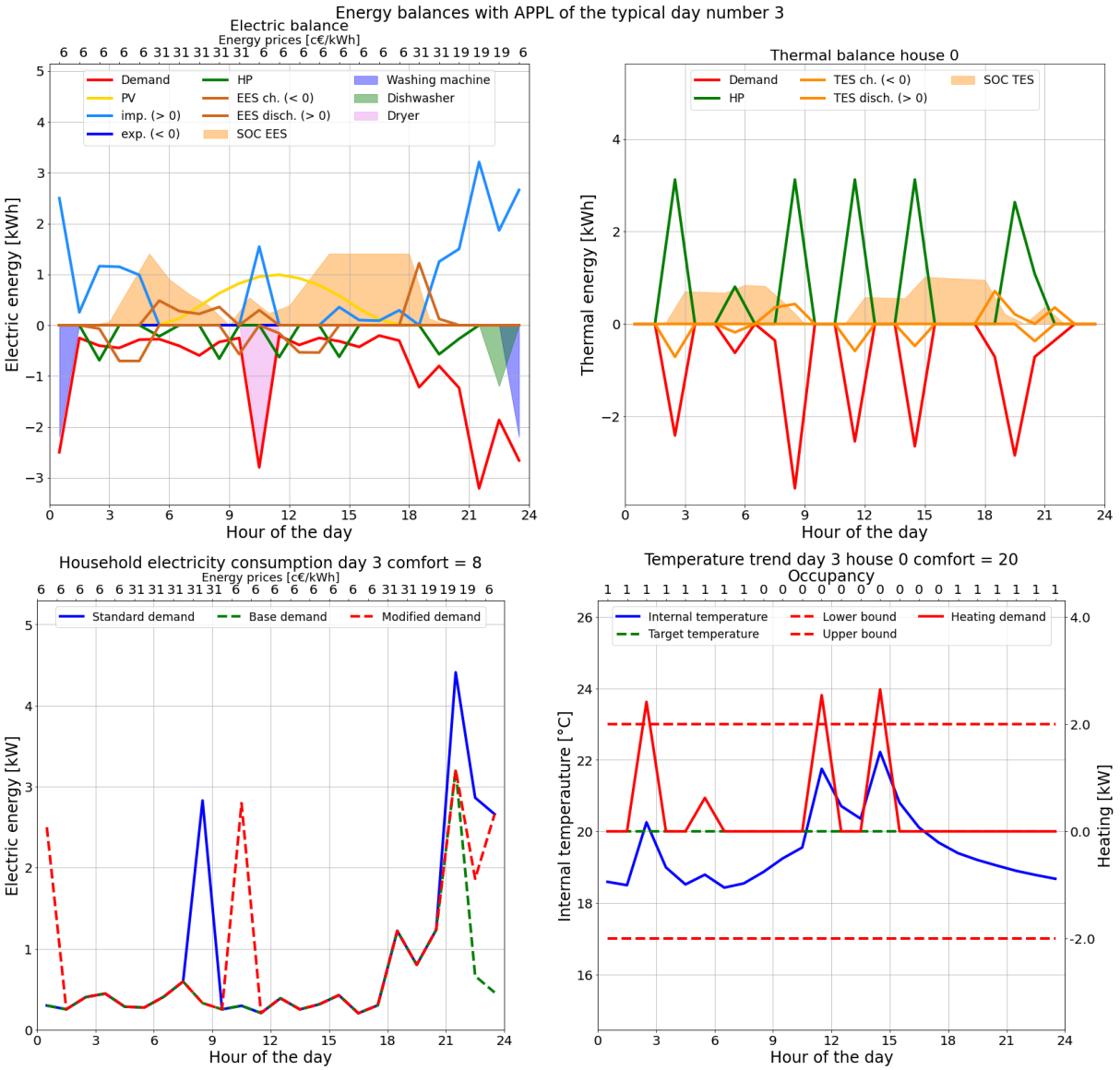

Figure 9: Typical fall day

For the fall day the strategy returns closer to the winter day, given the lower PV generation availability. The EES is employed to cover high electricity price hours, and is being charged in the morning from bought electricity and in the evening by excess PV generation. The appliance scheduling principle is the same as the winter day.
In the thermal balance, the HP is still being used at maximum capacity to exploit the best COP achievable, this is reflected also in the heating demand, which is concentrated in few hours instead of being low and constant during the whole day.

	Capacity
PV [kWp]	2,28
HP [kWth]	3,13
TES [kWh]	1,02
EES [kWh]	1,41

(a)

	Costs $[\frac{c€}{kWh}]$
COE_e	25,83
COE_t	19,65

(b)

Table 15: (a): Installed capacities of a single house under DR, (b): Costs of energy of a single house under DR

In the previous table it is possible to note the numerical results of the analysis. The PV capacity is moderate for a household (2,28 kWp). Only around 26% of the electricity produced by the PV is sold to the grid (defined in Equation 86) and about 24% of the electricity consumed by the household comes from the PV (defined in Equation 85). The HP size is roughly set (3,13 kWth), as the thermal demand does not vary greatly. Instead the installed capacities of the storages are both low (1,02 kWh for the TES and 1,41 kWh for the EES), as their main use is to provide help in achieving better cost performances, allowing the avoidance of high electricity prices or to allow generators to work efficiently, as can be observed in the previous graphs. The COE will instead provide a baseline of the costs for the next analyses and can also be compared to the same base case as in the previous analysis, subsection 3.1, where the electrical demand is satisfied by the grid and the thermal demand is satisfied by a natural gas boiler. The resulting COEs are, respectively 38.42$\frac{c€}{kWh}$ for the COE_e and 28.56$\frac{c€}{kWh}$ for the COE_t.

3.3 Comfort-savings analysis

To better understand the correlation between comfort and savings an iterative approach can be used to analyze all different comfort points.
Beginning with a broad analysis of the whole comfort spectrum, a surface graph can be produced for the variation of both comforts:

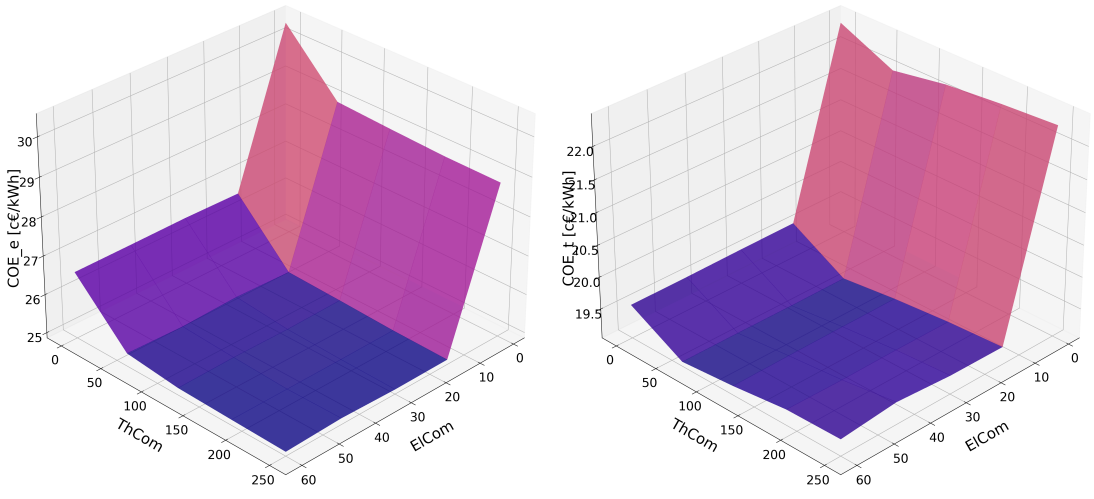

(a) (b)

Figure 10: Surface plot of the (a) COE_e and (b) COE_t under comfort variation

From these graphs, the most evident result is the predominant role of electrical comfort in driving the savings. Notably, there is a drop of approximately $4\frac{c€}{kWh}$ and $3\frac{c€}{kWh}$ for the COE_t and the COE_e respectively, as comfort shifts from the maximum to the minimum threshold. Although a decrease in thermal comfort does contribute to generating savings, the return is comparatively lower than that derived from a loss in electrical comfort, with variations in COE_t and COE_e amounting to around $2\frac{c€}{kWh}$ and $1\frac{c€}{kWh}$ respectively.
Both comfort exhibit a very sharp drop in COE in the first few degrees of the comfort loss and then tend to a minimum. To better observe this phenomena graphs featuring a narrower range of comfort variations are presented:

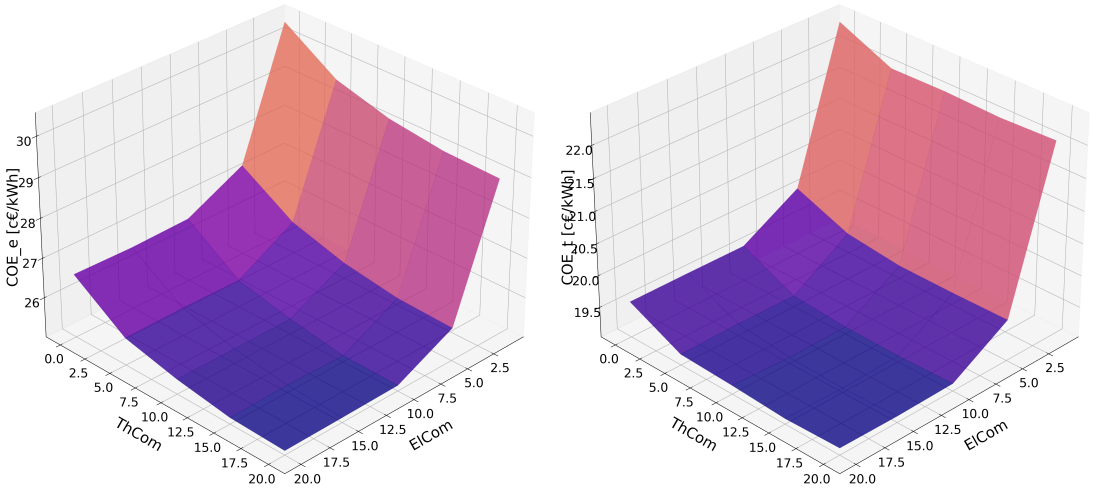

(a) (b)

Figure 11: Surface plot of the (a) COE_e and (b) COE_t under comfort variation

In this detailed version of the graphs, it is possible to observe that the electrical comfort loss is indeed the main driver in savings, characterized by a very sharp drop in COE in the first few degrees of comfort.
The thermal comfort also provides some savings, but it is more gradual. The plateau in COE seems to be already reached in this first few degrees of comfort loss.
To corroborate these findings, simplified graphs illustrating individual comfort-savings relationships are presented, to have a better definition of the cost-comfort front. These graphs were obtained respectively by fixing a thermal comfort of 20 and an electrical comfort of 6.

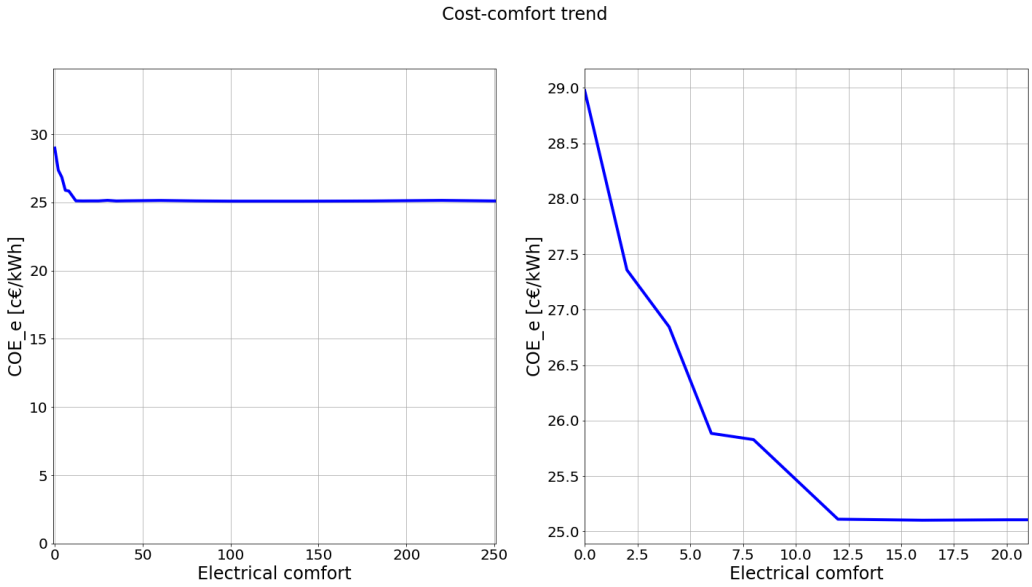

(a)

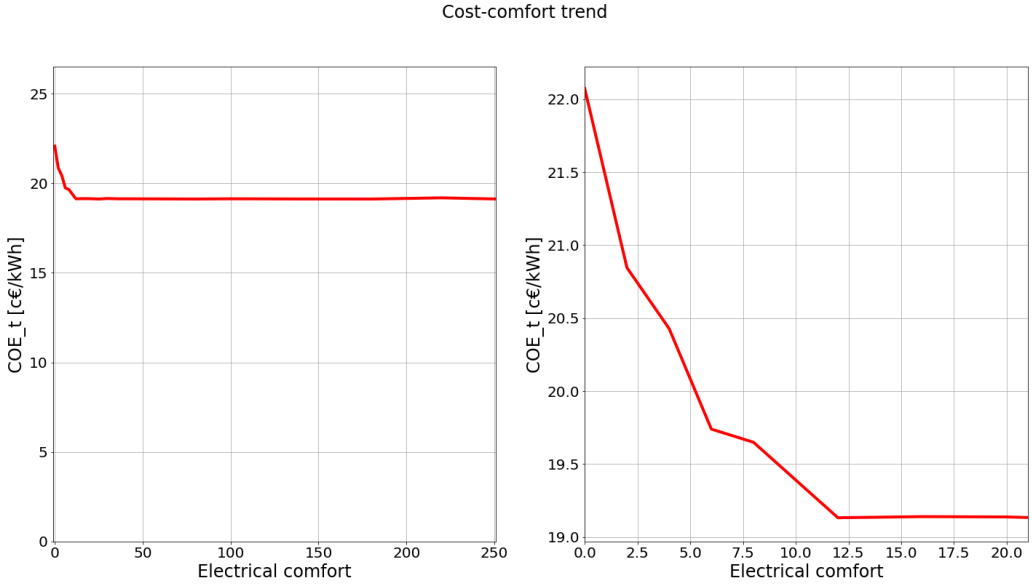

(b)

Figure 12: Electrical comfort-COE plot of the (a) COE_e and (b) COE_t

It can be noted that the trend is the same for the COE_e and the COE_t both, as the thermal load is a constant in this case (see Equation 83 and Equation 84). The COE flattens out near the minimum COE (respectively $25.10\frac{c€}{kWh}$ and $19.12\frac{c€}{kWh}$) already around the threshold of 12.
The value selected to represent the average user is 6, associated with a value of COE_e of $25.83\frac{c€}{kWh}$. This choice is motivated due to the fact that the trend is substantially a Pareto front and the value of 6 is the optimal value of compromise. Furthermore, while a higher value could potentially yield additional savings, the incremental comfort loss does not present a justified trade-off for the marginal gains.

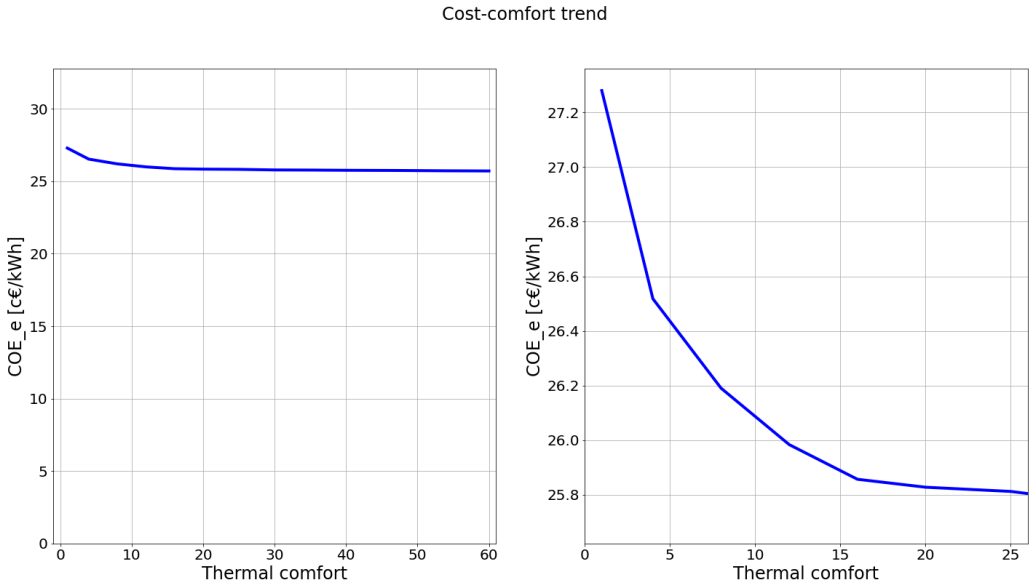

(a)

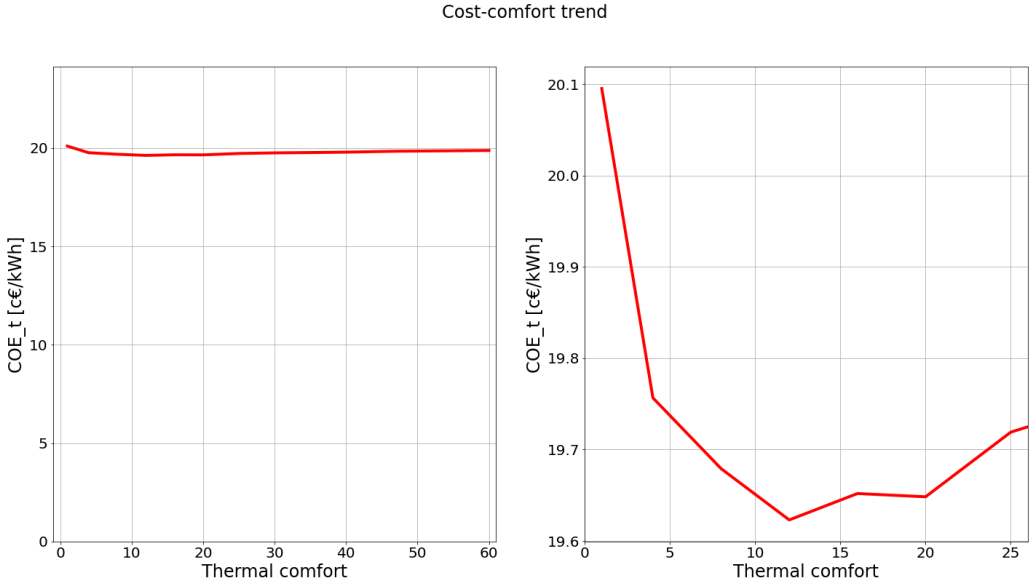

(b)

Figure 13: Thermal comfort-COE plot of the (a) COE_e and (b) COE_t

For the case of the thermal comfort, the trend is more gradual and reaches a plateau around the 20 threshold, associated with $25.83\frac{c€}{kWh}$ and $19.65\frac{c€}{kWh}$. This value is selected to represent the average user because, oppositely to the electrical comfort a variation in this value is less significant, as the temperature drops associated with the comfort loss are evenly spread out during the day and a minimum temperature is always guaranteed. Furthermore, the COE associated with the minimum comfort is a COE_e of $25.70\frac{c€}{kWh}$, meaning the savings available with further comfort loss are minimal.
Conversely, in the case of the COE_t the graph trends back up after reaching a minimum around 12, associated with $19.62\frac{c€}{kWh}$, this is due to how the COE_t is calculated (see Equation 84), where the thermal load is in the denominator. As the thermal comfort decreases, the thermal load also decreases, leading to an apparent increase in the COE_t. The COE for minimum comfort of 60 settles at a final COE_t of $19.87\frac{c€}{kWh}$.

3.4 Single houses EC analysis

In conducting this analysis, a maximum population of 6 households is set, as a trend still emerges from this analysis and the simulation time would otherwise be incompatible with the objective of the thesis. The comfort levels are uniformly set across all households, and is fixed to the thresholds of 6 for electrical and 20 for thermal.
The most significant graph is the following, as the COE is compared to the population of the EC:

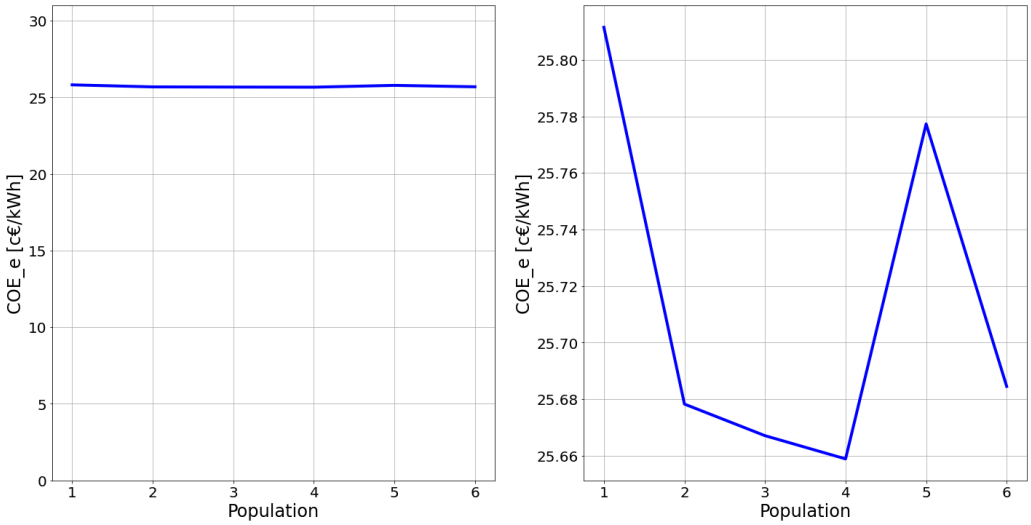

(a)

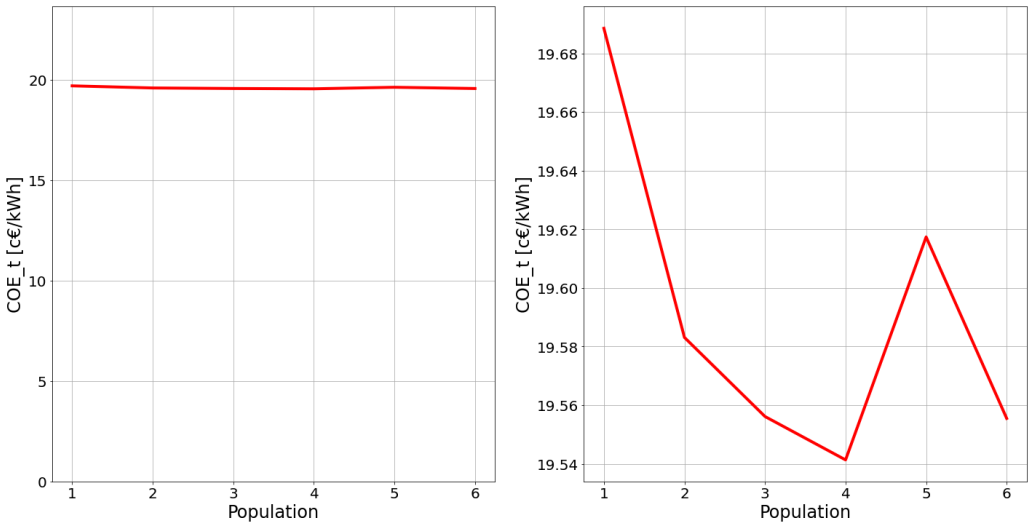

(b)

Figure 14: Population-COE plot of the (a) COE_e and (b) COE_t

As evident from the graphs, the COE shows a weak correlation with the population. Consequently, the process appears to be a scaled up version of the single household previously analyzed. This conclusion is corroborated by the graphs of the installed capacities in the EC as the population varies.

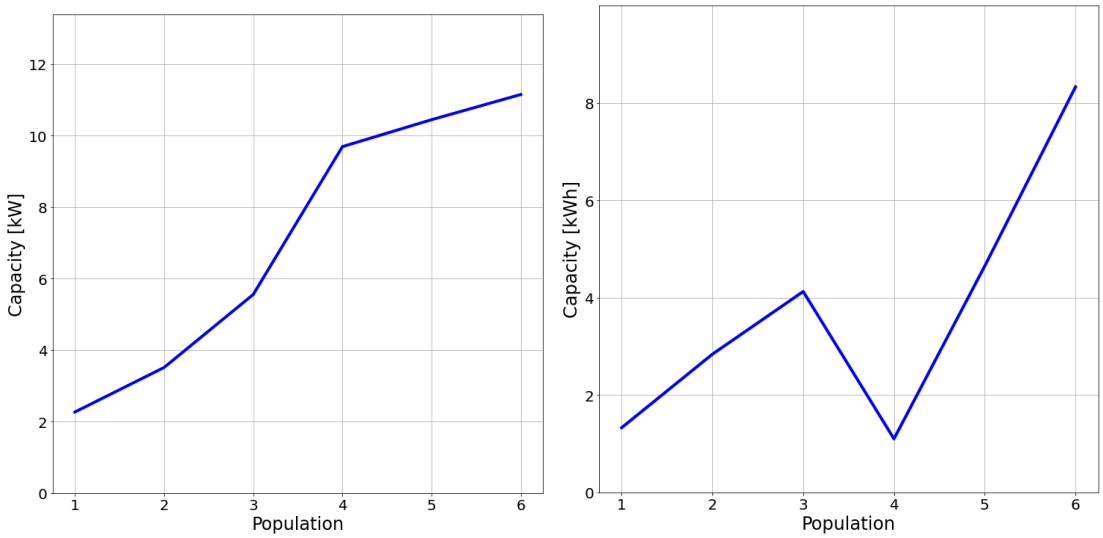

(a) (b)

Figure 15: Population-capacity plot of (a) PV and (b) EES

The marginal increase in PV capacity and concurrent decrease in EES capacity compensate each other, revealing a discernible linear increasing trend in the capacities.
This outcome conclusively establishes that an EC composed of households with the same comforts level does not yield any discernible economic advantage.
To assess whether uniform comfort levels across the entire EC is the determining factor, a subsequent simulation is conducted using six households with varying comfort thresholds. The comforts are [0, 0, 6, 6, 250, 250] for the electrical and [1, 1, 20, 20, 60, 60] for the thermal.
The results are the following:

Comfort	$COE_t \frac{c€}{kWh}$
[0,1]	20.92
[6,20]	20.21
[250,60]	19.95

Table 16: COE_t of an EC with varying levels of comfort

The COE_t is calculated with the relative energy consumption of each household, resulting in higher COE_t for households with greater comfort levels compared to those with lower comfort levels. Two observations arise from these results: the difference between a low comfort user and a high comfort user is marginal ($1\frac{c€}{kWh}$); secondly, the COE_t for this EC is at most equal or higher for every user compared to the previously analyzed EC, with a COE_t of around $19.56\frac{c€}{kWh}$.
For comparison, an EC composed only of household with comfort levels of 250 for electrical and 60 for thermal achieves a COE_e of $25.01\frac{c€}{kWh}$ and a COE_t of $19.32\frac{c€}{kWh}$.
The full trend of the COE is obtained through an ulterior analysis and the graph is provided:

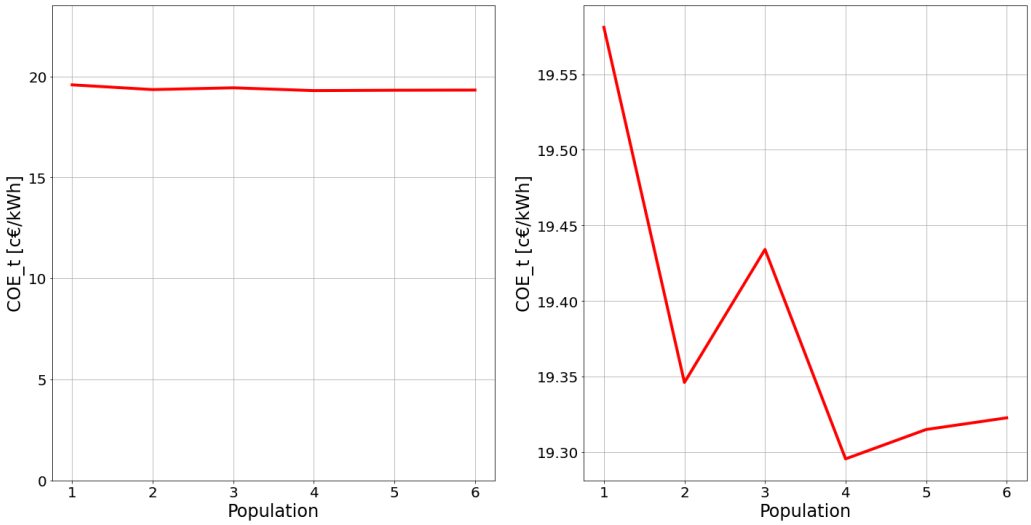

Figure 16: Population-COE_t plot with the lowest comfort level

It is evident that the comfort level does not change the result, as the graph shows the same trend but shifted downwards of around $0.2\frac{c€}{kWh}$.

3.5 Single houses EC with and without load shifting analysis

In this analysis, a maximum of 30 households without load shifting is set, represented in the graphs as the population. The households with load shifting have their comfort levels set to 6 for electrical and 20 for thermal. The first iteration is started with a single household with load shifting and the COE trends are the following:

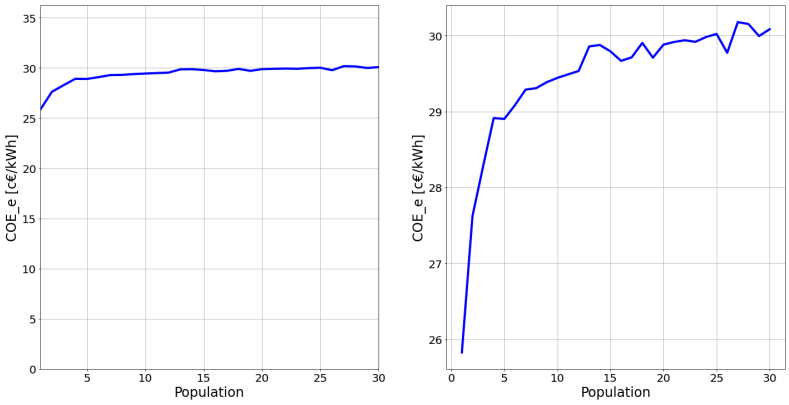

(a)

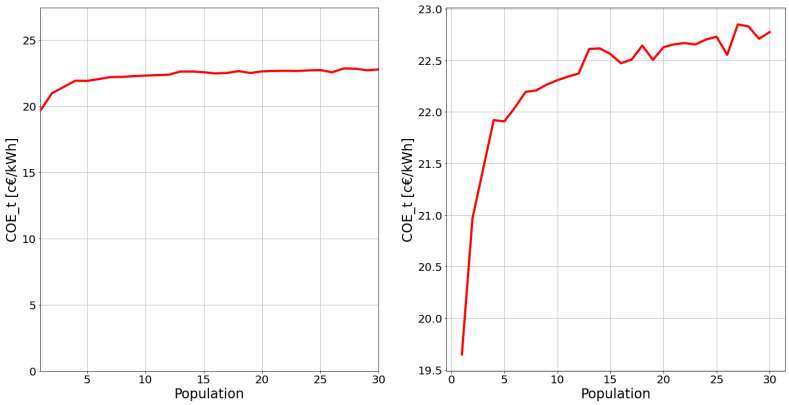

(b)

Figure 17: Population-COE plot of the (a) COE_e and (b) COE_t

It is possible to observe that the COE shows an increasing trend, leading to an asymptote around $31\frac{c€}{kWh}$ for the COE_e and $23\frac{c€}{kWh}$ for the COE_t. This indicates that no substantial advantage is derived from this aggregation of households.
To investigate whether the comfort levels of households with load shifting capabilities influence the results, another analysis was conducted with minimum comfort levels:

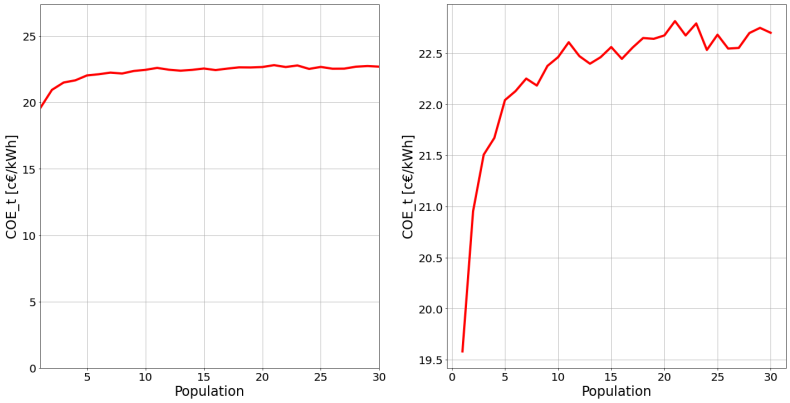

Figure 18: Population-COE_t plot with minimum comforts

No meaningful difference can be noticed, so it is safe to assume that for this combination even the comfort does not play a role in the trend of the COE.
Next, one more user with load shifting is added to the EC to perform another analysis:

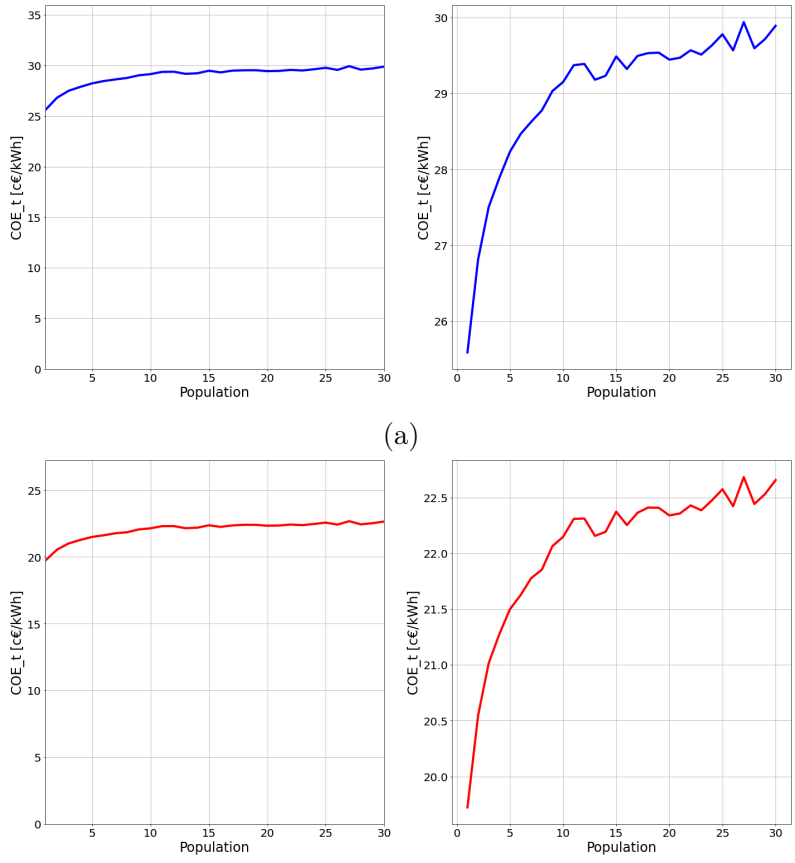

Figure 19: Population-COE plot of the (a) COE_e and (b) COE_t

Both graphs show a marginal reduction compared to the case with only one house with load shifting, as the maximum is now around 30 $\frac{c€}{kWh}$ for the COE_e and around 22.7 $\frac{c€}{kWh}$ for the COE_t. However, the overall trend remains consistent with the previous case. Again, a new simulation with the two users with the minimum level of comforts is performed to ensure that comfort does not play a role in determining the COE-population trend.

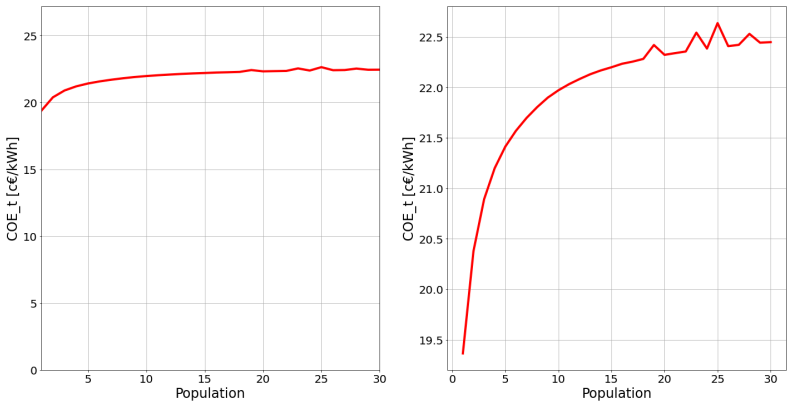

Figure 20: Population-COE_t plot with minimum comforts

Even in this case no meaningful difference can be discerned over the previous case, as the COE_t still tends to the same maximum value of around $22.5 \frac{c€}{kWh}$.
One final analysis is performed with 3 users with load shifting to ascertain the effect of the number of users with load shifting.

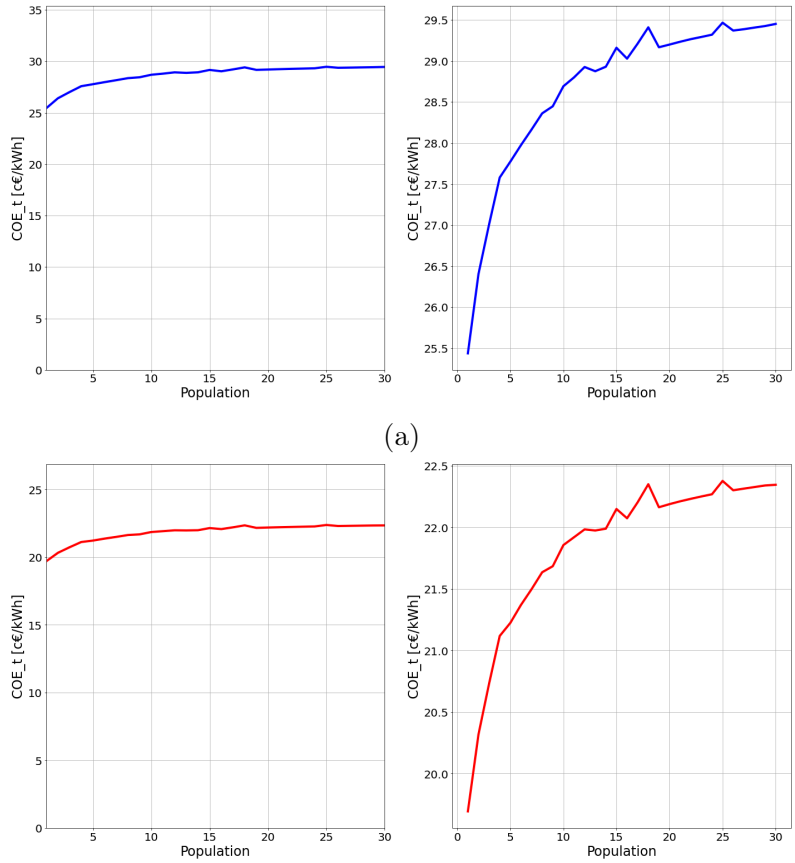

Figure 21: Population-COE plot of the (a) COE_e and (b) COE_t

Also in this case the trend increases up to a maximum, even though the maximum value decreases as the number of users with load shifting increase. This effect is still not enough to counteract the increase of the COE as the number of household without load shifting increases.

3.6 Residential users and industrial user EC

In this analysis, the residential users can load shift and have standard comfort levels of 6 for electrical and 20 for thermal. The trend for the COE of the EC is the following, where the population denotes the number of households:

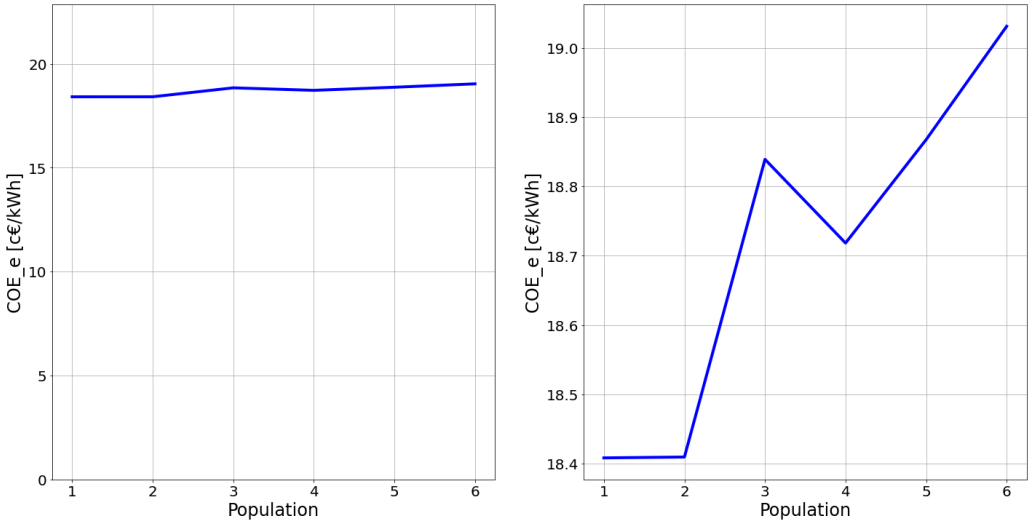

(a)

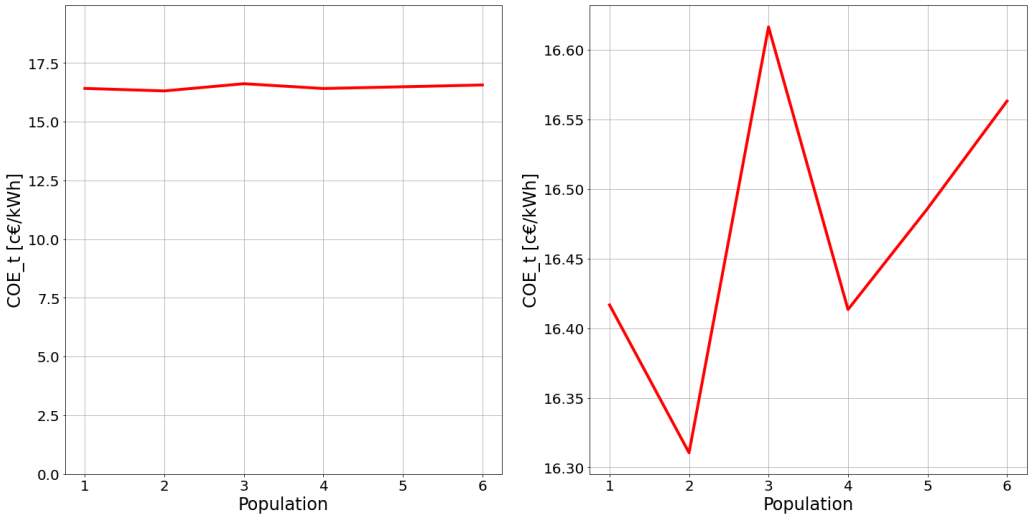

(b)

Figure 22: Population-COE plot of the (a) COE_e and (b) COE_t

If the absolute values of the COE are compared to the single household, at first glance, this type of EC seems very convenient, but it must be also observed that the trend of the COE is only slightly increasing and just starts from a low value. This is most likely due to the significant difference in loads between the household and the industrial user. To verify this, a simulation with the same parameters as the one performed in subsubsection 2.4.2 is carried out considering only the industrial user with no ability to shift its loads. The results are the following:

	Capacity
PV [kWp]	63.96
HP [kWth]	29.63
TES [kWh]	38.84
EES [kWh]	44.10

(a)

	Costs $[\frac{c€}{kWh}]$
COE_e	18.23
COE_t	16.35

(b)

Table 17: (a): Installed capacities of an industrial user, (b): COE of an industrial user

As it is possible to observe, the COE for the industrial user alone is close to the COE for the EC, due to the magnitude of the load of the industrial user driving the COE down alone. This suggests that there is minimal advantage for the industrial user in forming an EC with households capable of load shifting, while the households would experience significant benefits (a single household achieves a COE_e of $25,83\frac{c€}{kWh}$ and a COE_t of $19,65\frac{c€}{kWh}$).

Another simulation was conducted with low-comfort users to assess if changes in the comfort levels of residential users make a difference:

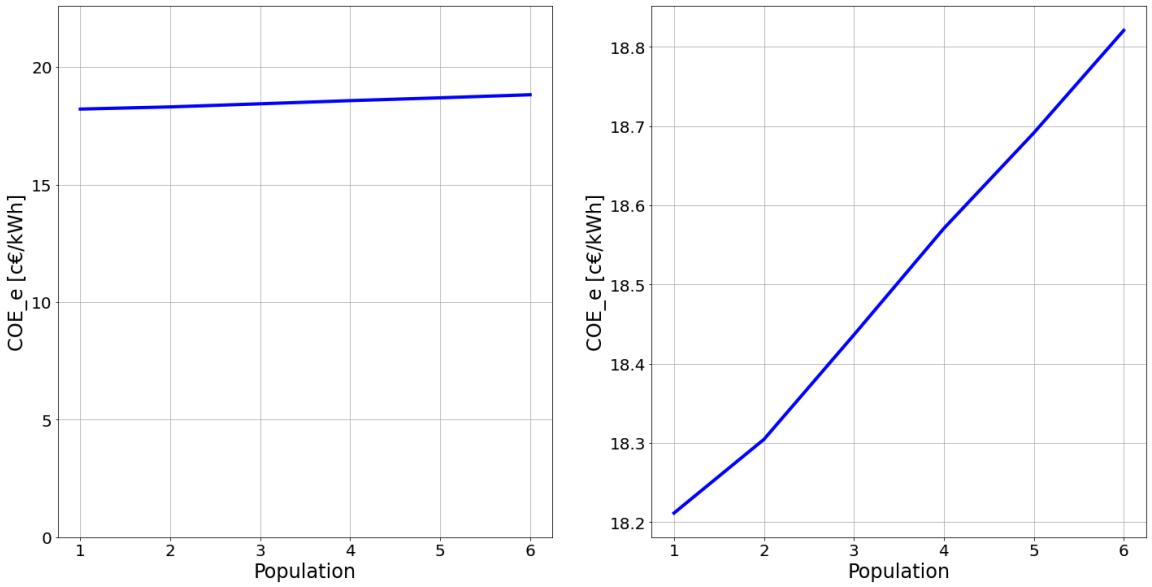

(a)

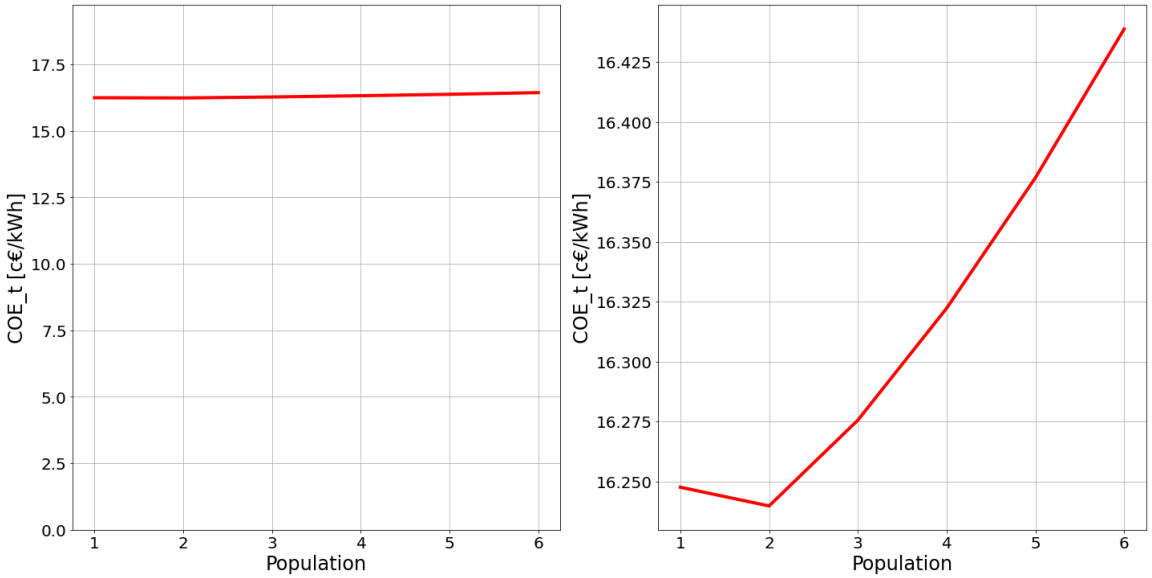

(b)

Figure 23: Population-COE plot of the (a) COE_e and (b) COE_t

From the results observable from the graph it is even clearer that an EC of an industrial user with residential users under this conditions is not convenient. As the population increases, so does the COE, indicating no economic benefits.

3.7 Residential users with and without load shifting and industrial user EC

The analyses are carried out by fixing the number of users with load shifting, keeping the industrial user as one fixed load and by varying the number of household without load shifting. The first analysis performed is carried out with only one household capable of load shifting, and the trend of the COE are the following:

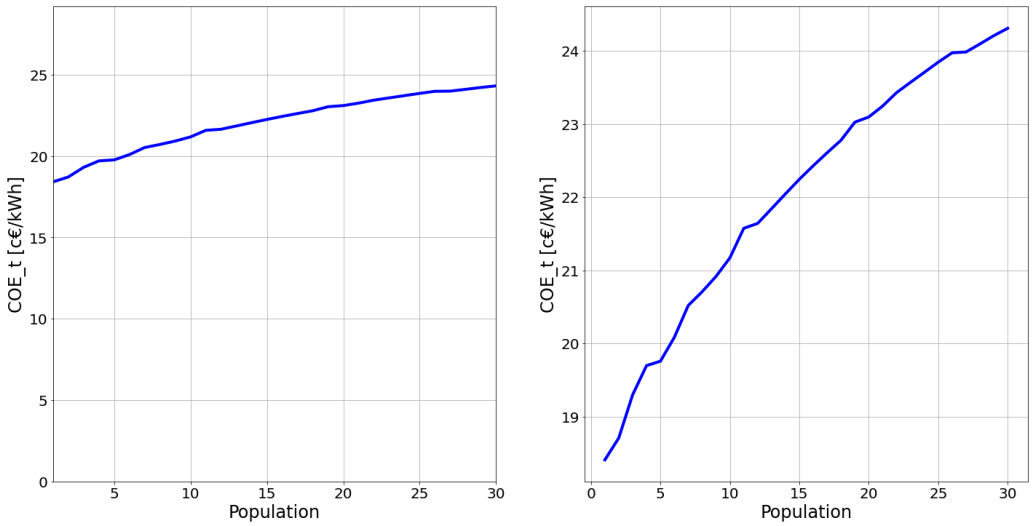

(a)

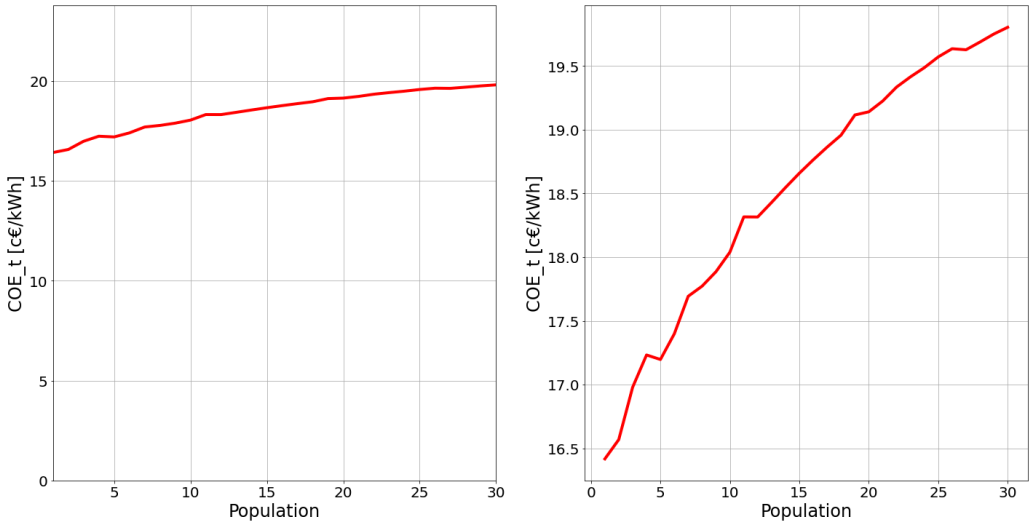

(b)

Figure 24: Population-COE plot of the (a) COE_e and (b) COE_t with one load-shifting user

Remembering that the COE for the industrial user alone is respectively $18.23\frac{c€}{kWh}$ for the COE_e and $16.35\frac{c€}{kWh}$ for the COE_t, the COE increases with the population.
This analysis is repeated after adding another residential user capable of load shifting.

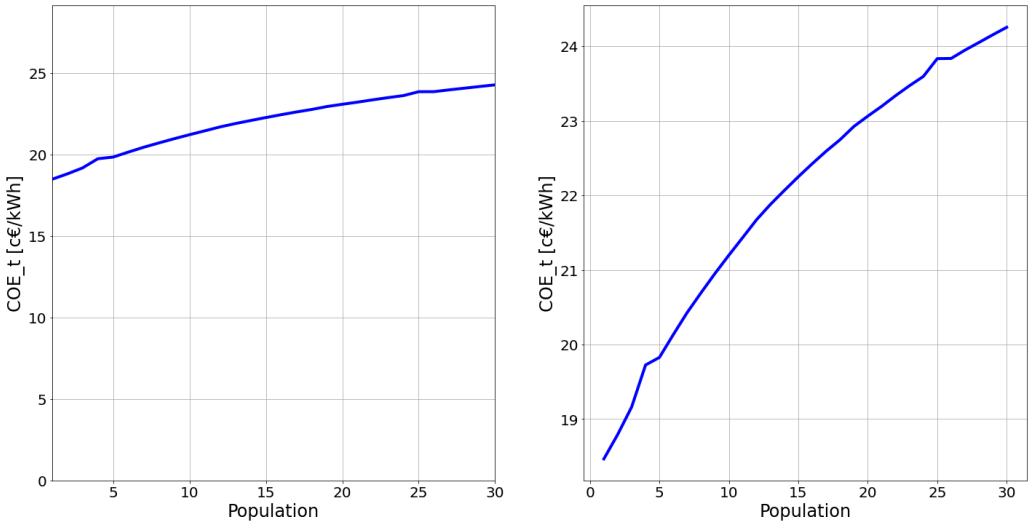

(a)

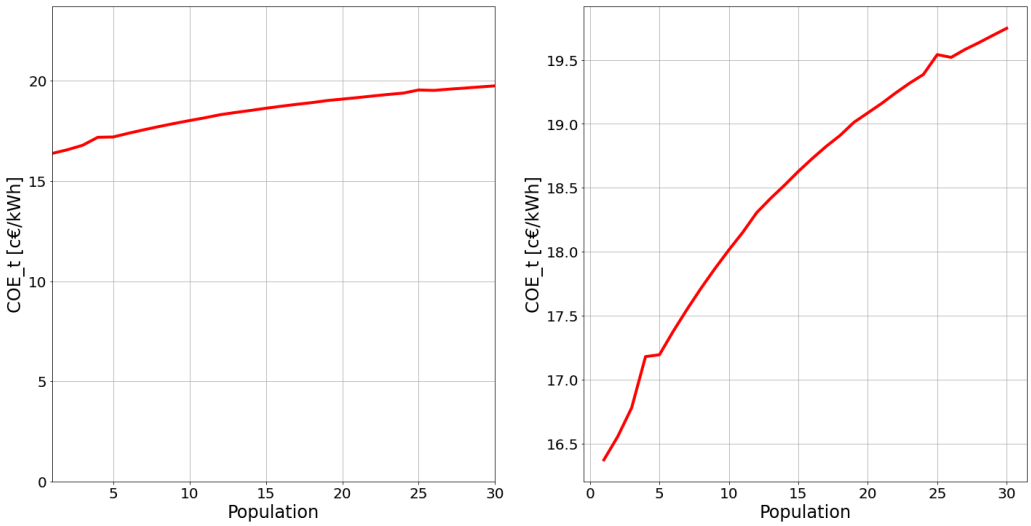

(b)

Figure 25: Population-COE plot of the (a) COE_e and (b) COE_t with two load-shifting user

It is possible to observe that the inclusion of an additional user has minimal impact, as the trend is mostly identical to the previous analysis. To confirm whether the addition of households capable of load shifting induces any notable changes in the COE trend, one more analysis is performed with three users with load shifting capabilities.

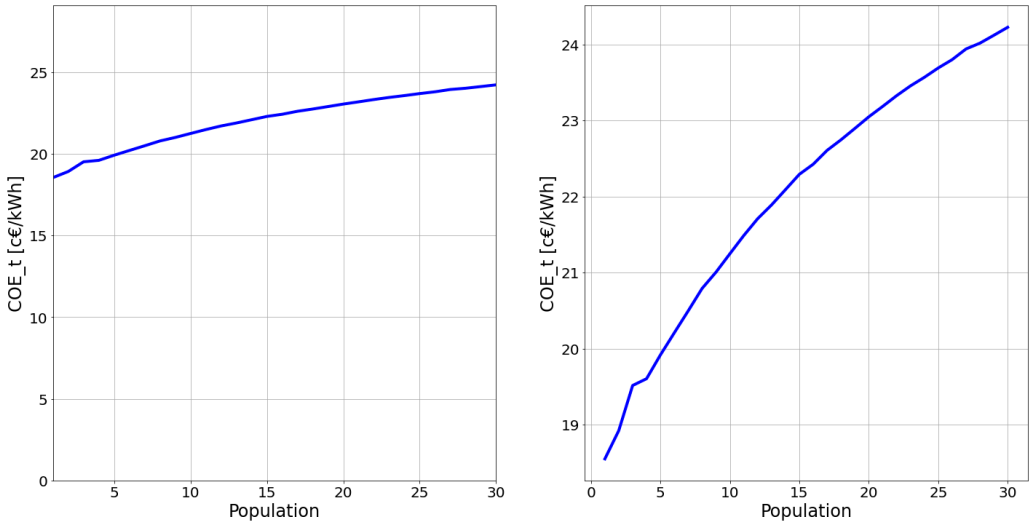

(a)

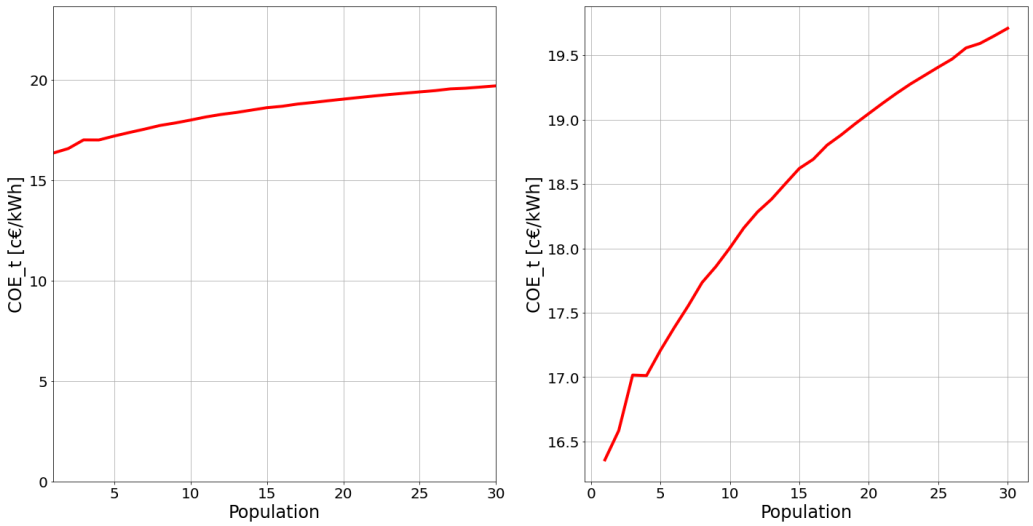

(b)

Figure 26: Population-COE plot of the (a) COE_e and (b) COE_t with three load-shifting user

Even in this analysis the trend remains the same, both for the COE_e and the COE_t. To ascertain if the comfort levels produce a variation in the population-COE trend, the same three cases are performed with all the load shifting capable users set at the minimum comfort level.

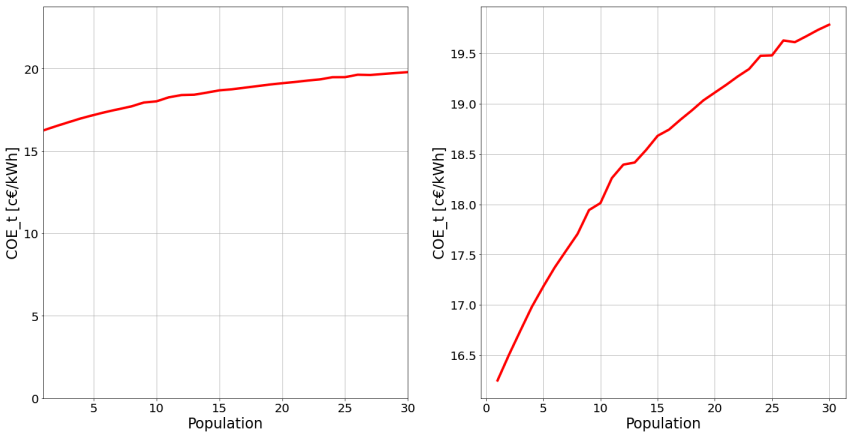

(a)

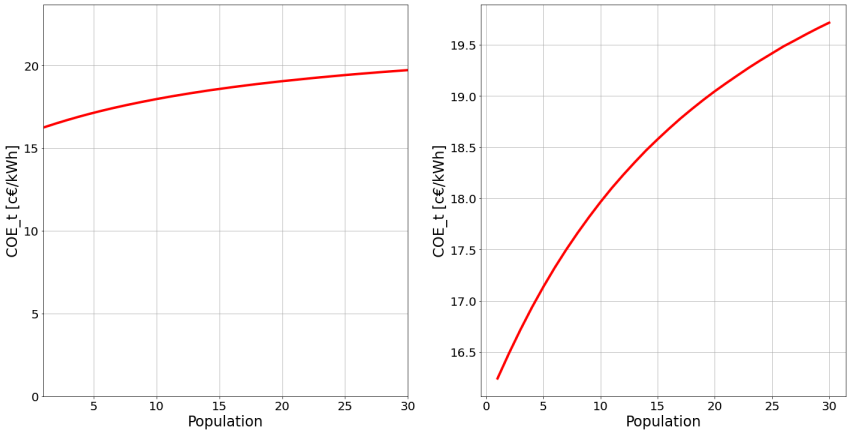

(b)

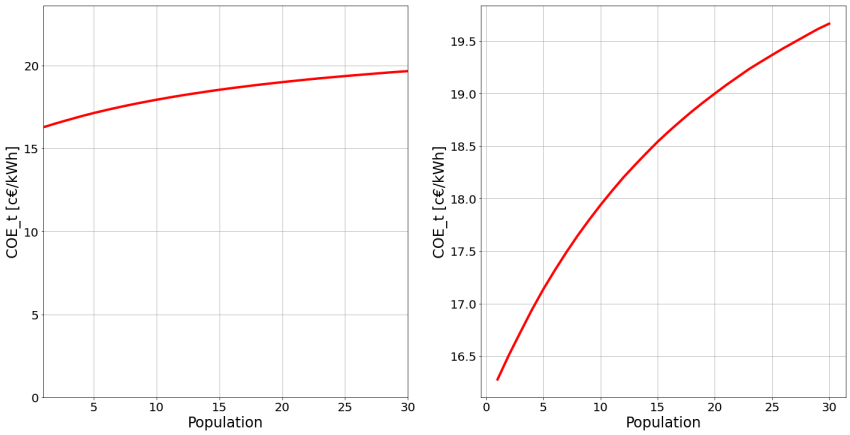

(c)

Figure 27: Population-COE_t plot with (a) one,(b) two and (c) three users capable of load shifting with minimum comfort levels

Even in this case the addition of users with load shifting capabilities brings almost no change in the COE trend, as the trend stay the same aside from a minor decrease in absolute value.

3.8 Sensitivity analysis

The chosen model where the sensitivity analyses are carried out is the one described in subsubsection 2.4.2, where the comfort levels are set to 6 for the electrical comfort and to 20 for the thermal comfort.
To provide a quick overview of the sensitivity analyses, the most relevant results will be shown first and in the last part a brief section will be dedicate to all parameters that instead produce a linear variation.
Following the same order as Table 12, the first notable variable is $f_{heat,rad}$:

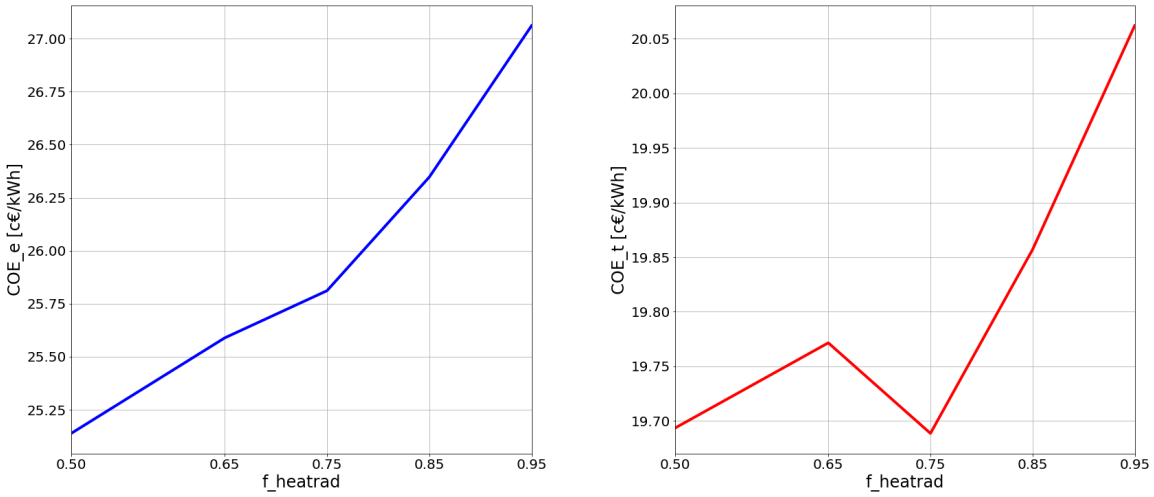

(a) (b)

Figure 28: $f_{heat,rad}$ plot against the (a) COE_e and the (b) COE_t

Diminishing the fraction of heat diffused through radiative heating shows a direct correlation with the COE. To further understand the following graphs are presented:

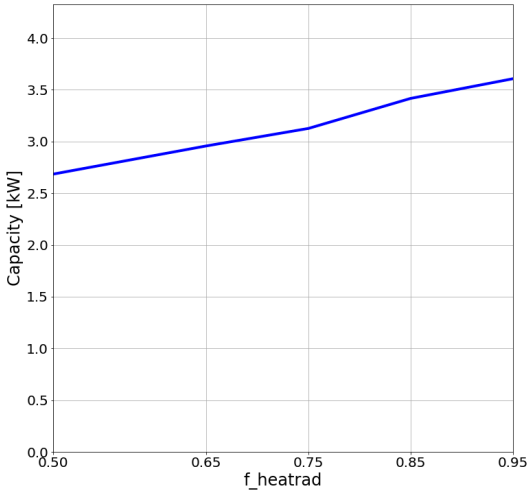

(a)

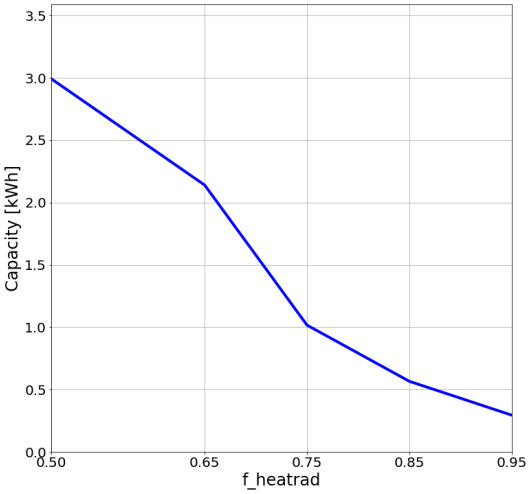

(b)

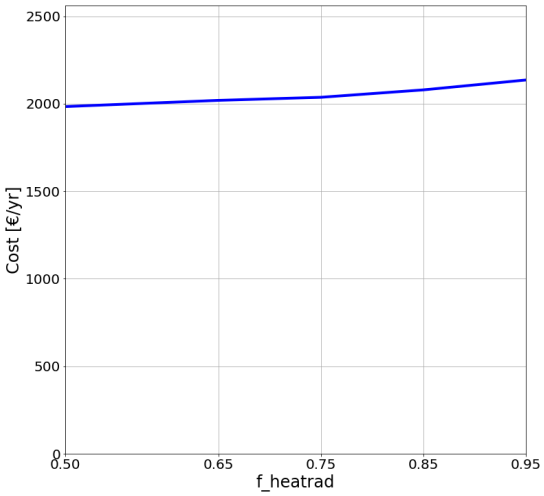

(c)

Figure 29: $f_{heat,rad}$ plot against the (a) HP capacity, the (b) TES capacity and the (c) sum of $Cost_{INV}$ and $Cost_{OP}$

As the $f_{heat,rad}$ increases the capacity of the HP increases as well, while the TES decreases. This is due to the walls acting as a storage because the heat is flowing almost directly through them. The yearly costs then increase slightly producing an overall increase in the COE.
Following, the analyzed variable is d_W

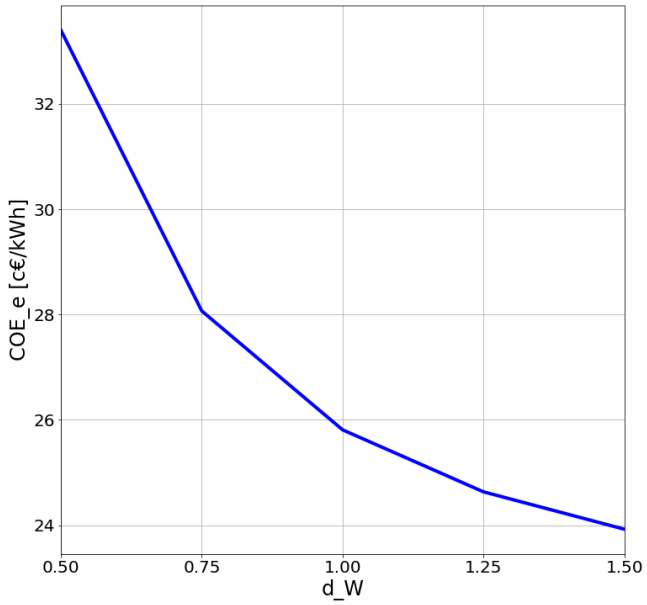

(a)

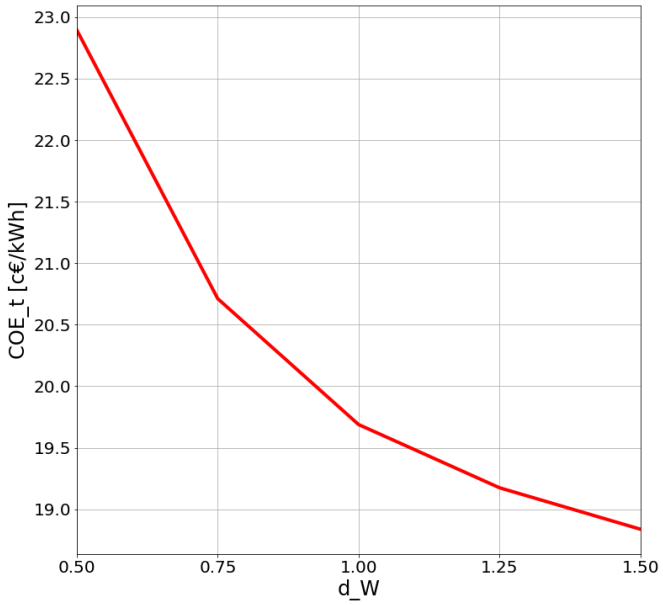

(b)

Figure 30: d_W plot against the (a) COE_e and the (b) COE_t

As it is possible to expect as the wall thickness increases the COE decreases, due to the house being better insulated from the exterior. The trend is seemingly quadratic, as increasing the wall thickness provides diminishing returns. To observe the effect on the capacities more graphs are printed:

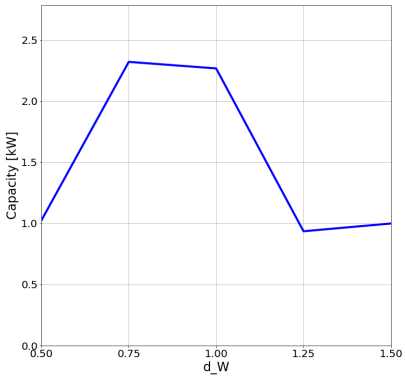

(a)

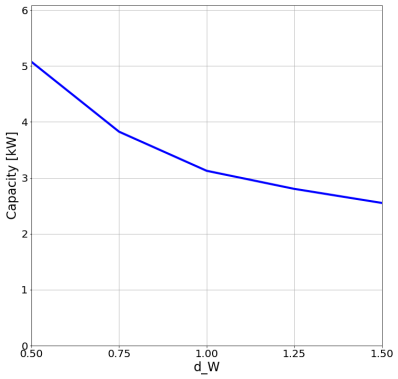

(b)

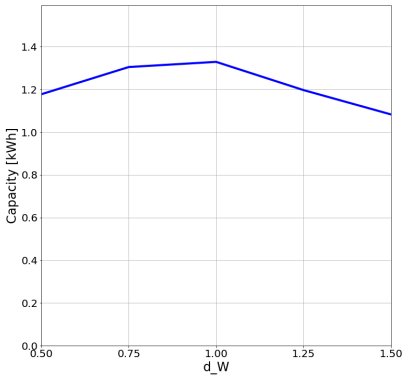

(c)

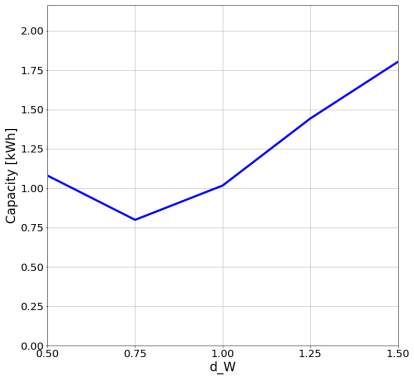

(d)

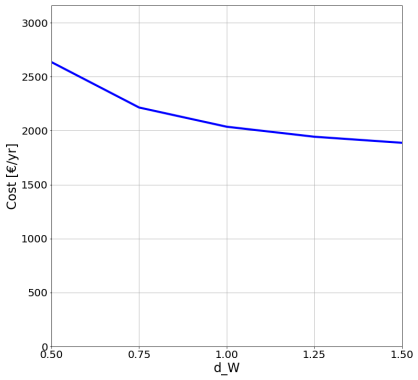

(e)

Figure 31: d_W plot against the (a) PV capacity, the (b) HP capacity, the (c) EES capacity, the (d) TES capacity and the (e) sum of $Cost_{INV}$ and $Cost_{OP}$

It is possible to observe that the PV and the EES capacity follow the same trend more or less, with a higher capacity for 0.75 and 1 d_W and lower capacity for the rest. Instead the HP and the EES capacities have a mostly inverse correlation, with the HP following as expected a quadratic trend. The yearly costs have a low slope downwards, as the higher wall thickness allow for overall lower investments in installed capacities.

The next variable analyzed is the starting times of the appliances, but analyzing only a few values gave little insight to the effective variation in the COE. Therefore, a complete graph of all possible variations is provided:

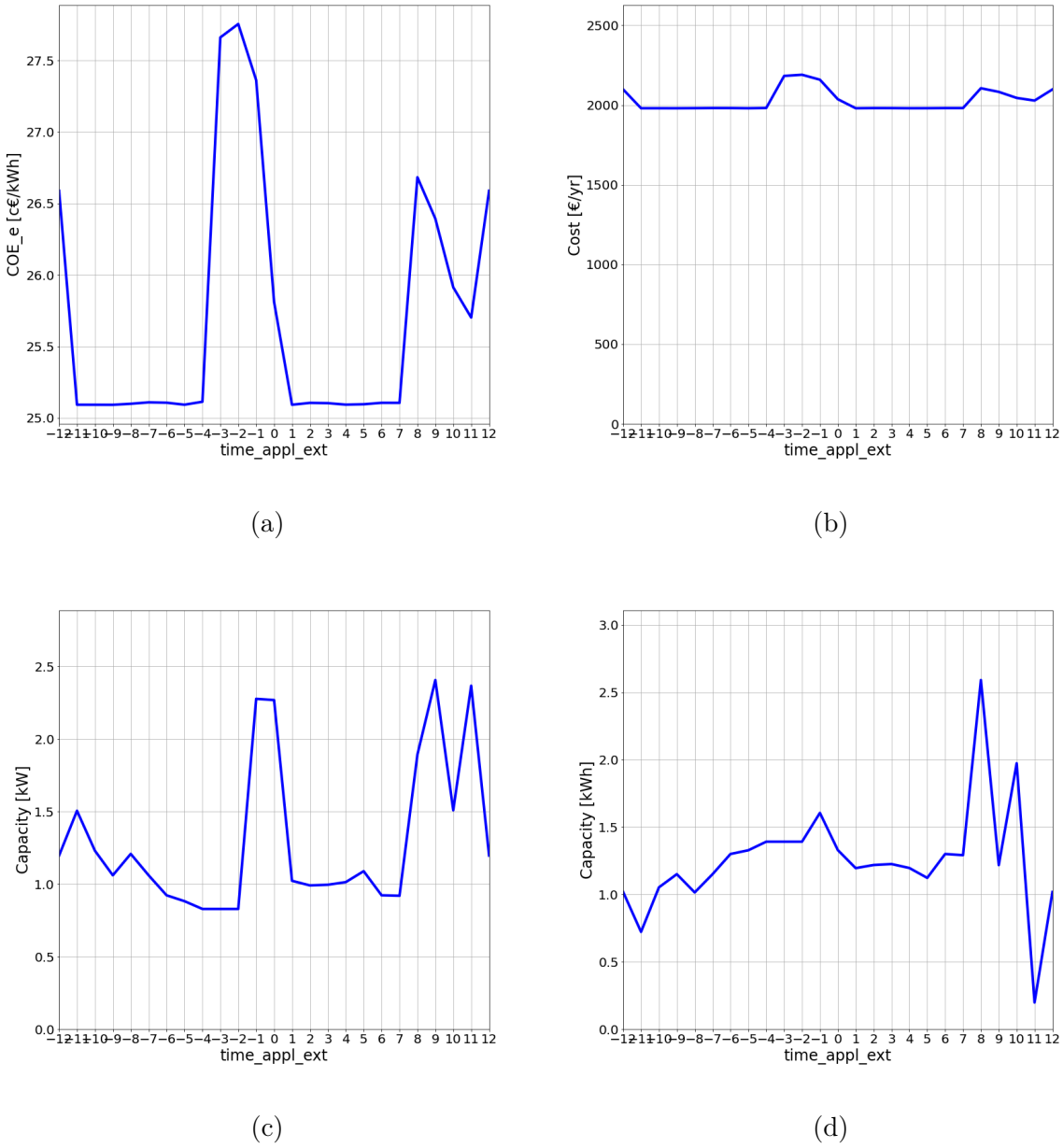

(a) (b)

(c) (d)

Figure 32: $time_{appl}$ plot against the (a) COE_e, the (b) sum of $Cost_{INV}$ and $Cost_{OP}$, the (c) PV and the (d) EES capacities

It is possible to observe that the COE decreases of around $0.5\frac{c€}{kWh}$ with a simple shift forward of one hour of the target start-up time of the appliances. This effect is mostly due to the selected starting time of the dishwasher and washing machine, respectively 21 and 22, being on the edge of middle price hours. The shift forward would schedule these two appliances in low price hours, allowing the optimizer to focus the electrical comfort in shifting the dryer. This effect allows the reduction in PV and EES capacity, leading to even further savings.

Another analysis on the time is performed, combining all three time factors: appliances starting time, DHW request time and occupancy. The following graphs are the result:

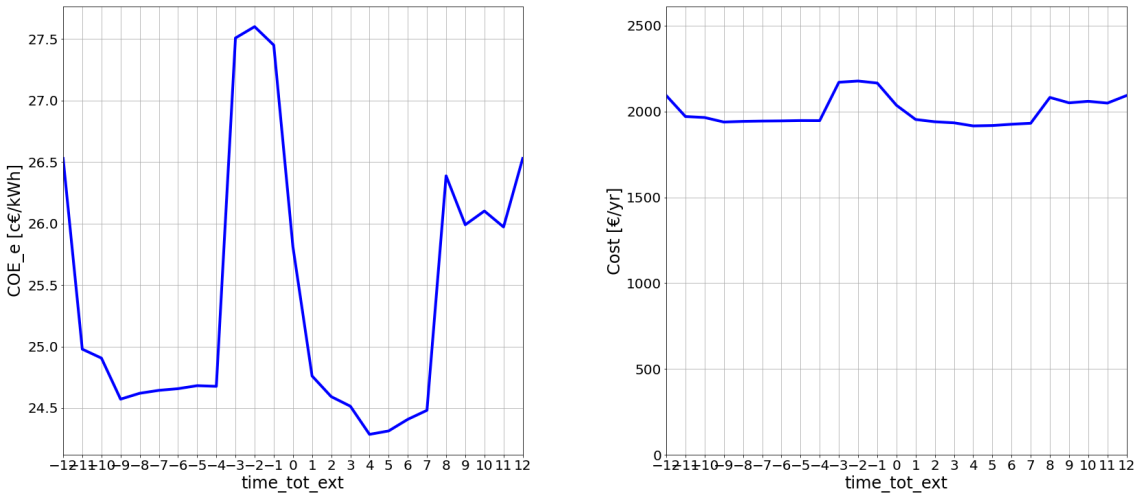

(a) (b)

Figure 33: $time_{tot}$ plot against the (a) COE_e and the (b) sum of $Cost_{INV}$ and $Cost_{OP}$

It is apparent that the trend is very similar, but the overall value of the COE is lower. The minimum in the COE is now at a four hour shift forward with a COE_e of around $24.25\frac{c€}{kWh}$, but with just a shift forward of one hour the COE_e already reaches around $24.75\frac{c€}{kWh}$, from the initial $25.63\frac{c€}{kWh}$.
Next, the results of the sensitivity analysis for the T_{amb} are the following:

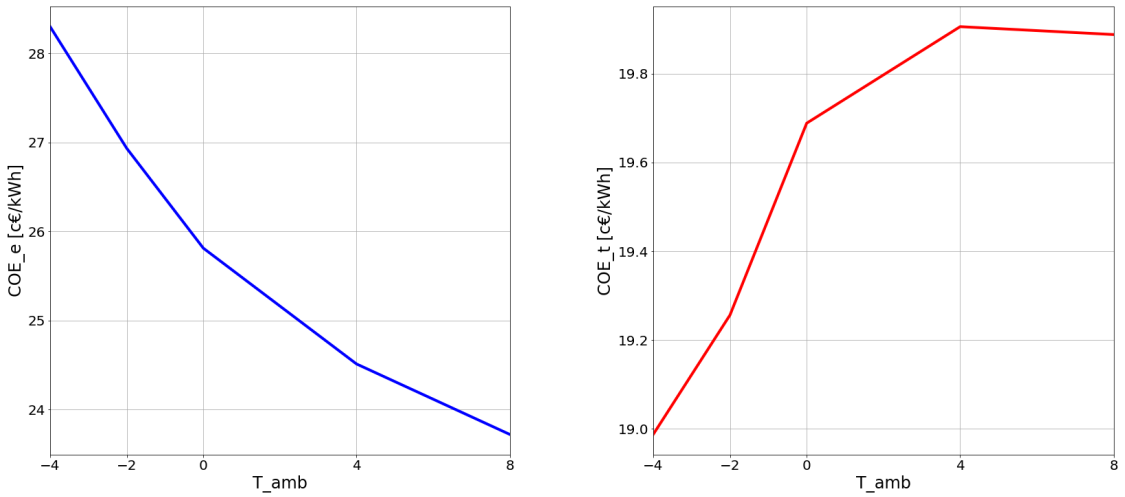

(a) (b)

Figure 34: T_{amb} plot against the (a) COE_e and the (b) COE_t

The two COEs seem to have opposite trends, but remembering their definitions (Equation 83 and Equation 84) the difference is in the inclusion of the thermal load, which increases as the ambient temperature is lower and decreases as the ambient temperature is higher. To better understand how the system changes graphs of the capacities and the total costs are showed:

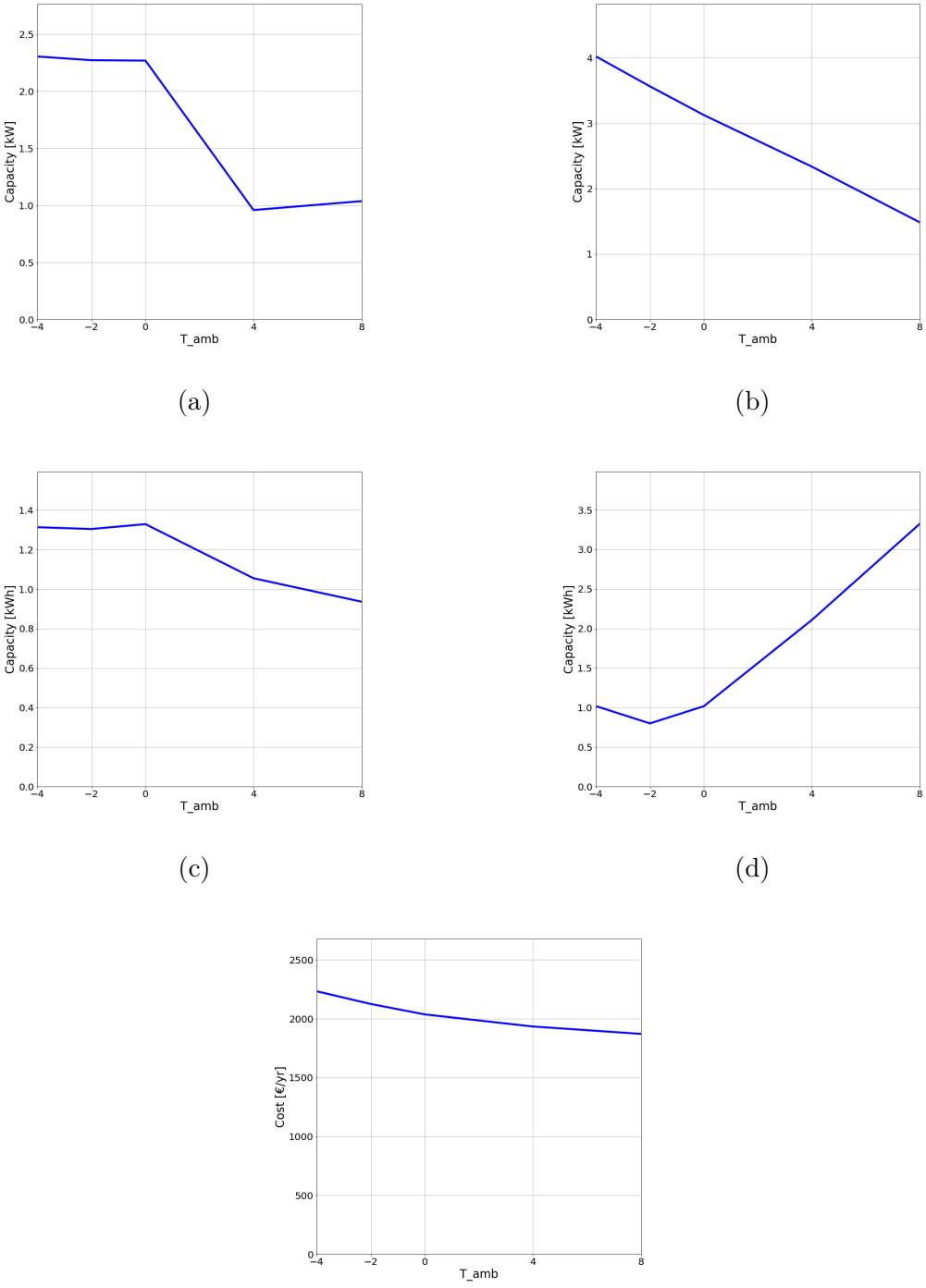

Figure 35: T_{amb} plot against the (a) PV capacity, the (b) HP capacity, the (c) EES capacity, the (d) TES capacity and the (e) sum of $Cost_{INV}$ and $Cost_{OP}$

It is evident that for lower ambient temperature the installed capacities are higher, except for the TES. This is mostly due to the HP size, because as it increases, the need for storage decreases, as the HP works constantly during the day lowering the need for storage.
The total costs also decrease with the ambient temperature, rising sharply instead as the ambient temperature decreases.
The last variable to produce a non linear change is the SolRad:

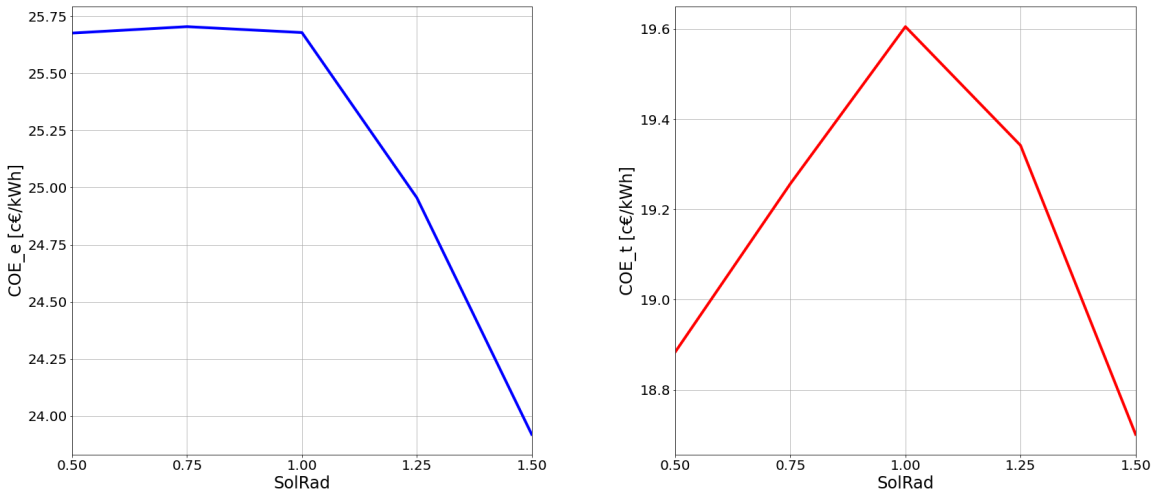

(a) (b)

Figure 36: $cbuy_{el}$ plot against the (a) COE_e and the (b) COE_t

The two graphs show contrasting trends, but as stated previously the COE_t accounts for the thermal demand, so it makes sense that as the solar radiation decreases the COE_t decreases, especially since for the same values the COE_e is stationary.

Another interesting effect is on the installed capacities:

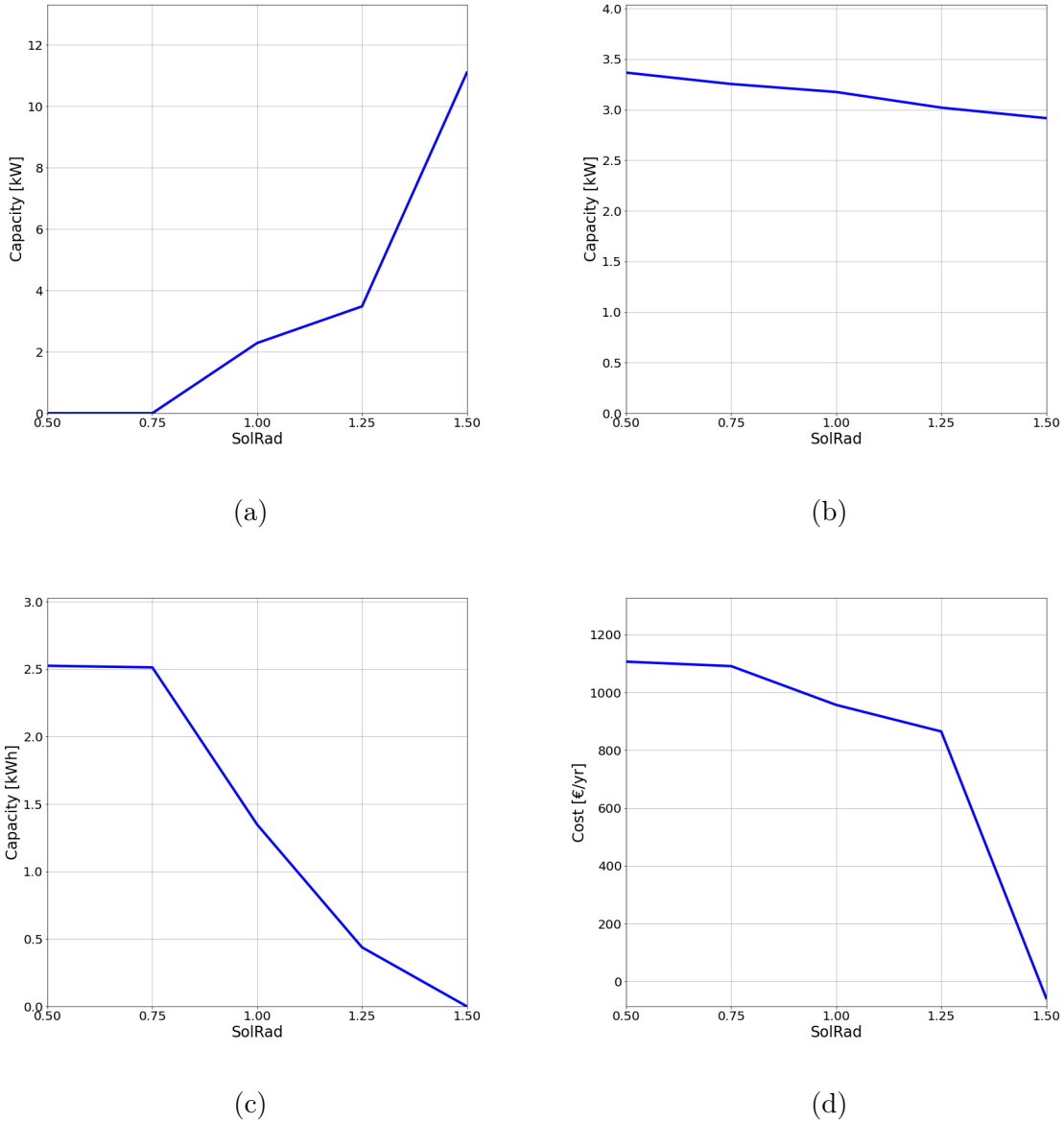

Figure 37: SolRad plot against the (a) PV, (b) HP and (c) EES capacities and the (d) $Cost_{OP}$

As the solar radiation increases the installed PV increases rapidly, as the produced energy depends directly from the solar radiation. For this reason the operation costs reach a negative value when the solar radiation is 1.5 times the normal value.
Contrary to the other analyses, the EES capacity does not correlate directly with the PV. In this case it is inversely proportional. This is due to the fact that the PV capacity is zero for reduced solar radiation, so the optimizer utilizes the EES to store electricity during high electricity prices hours, while for high solar radiation the installed PV capacity is high enough to not require any storage.
The HP also decreases slightly as the solar radiation helps reduces the heating load during the heating season.

Before starting the section of the linear variables, another variable is presented, T_{target} (both the winter and summer target temperature are changed):

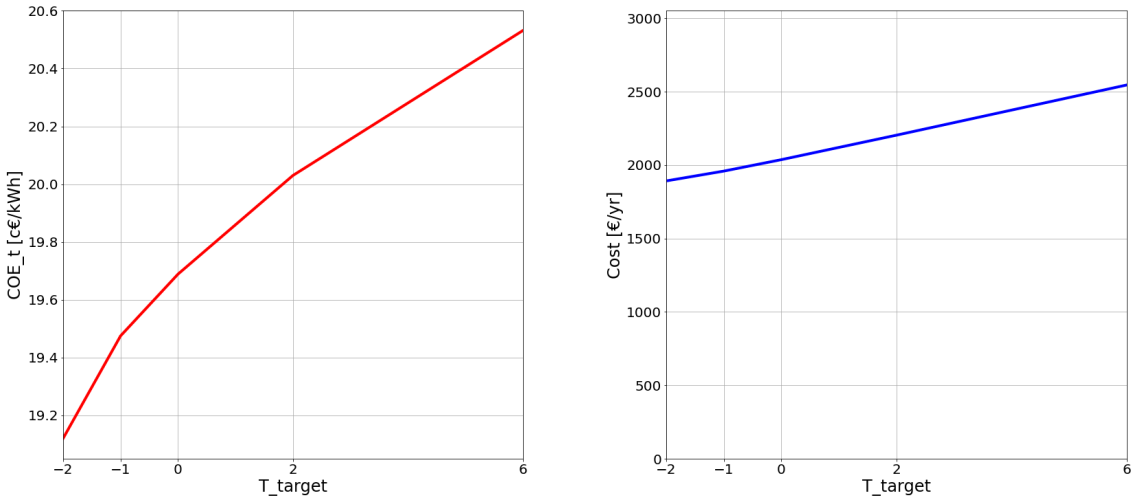

(a) (b)

Figure 38: T_{target} plot against the (a) COE_t and the (b) sum of $Cost_{INV}$ and $Cost_{OP}$

As one might reasonably assume the COE increases with the target temperature, but it also showed that the actual yearly costs show a linear trend, as the capacities installed are fitted to the specific case.
As for the parameters associated with linear results, first a list is provided:

Variable	Unit
$cbuy_{el}$	$[\frac{c€}{kWh}]$
$cbuy_{el}$ and $csell_{el}$	$[\frac{c€}{kWh}]$
Investment costs	[€]
Interest rate r	-
f_{sol}	-
h_f	-
h_A	-
V_{house}	$[m^3]$
n_{air}	$[h^{-1}]$
V_{DHW}	$[\frac{m^3}{day}]$
λ_{wall}	$[\frac{W}{m^2 \cdot K}]$
ρ_{wall}	$[\frac{kg}{m^3}]$
$c_{p,wall}$	$[\frac{J}{kg \cdot K}]$
time of DHW	$[h]$
occupancy	$[h]$

Table 18: Parameters associated with linear results

Some of the most interesting variables will be presented. Starting from $cbuy_{el}$:

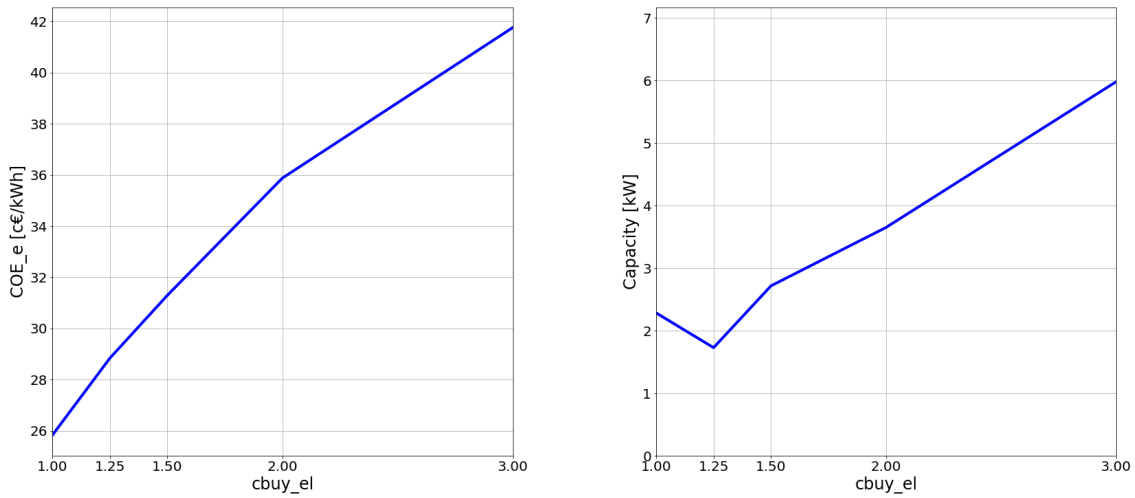

(a) (b)

Figure 39: $cbuy_{el}$ plot against the (a) COE_e and the (b) PV capacity

The COE is mostly linear, rising rapidly with cost of electricity. The interesting effect is an increase in installed PV capacity to compensate the high electricity prices. Another interesting variable analyzed is the combination of $cbuy_{el}$ and $csell_{el}$:

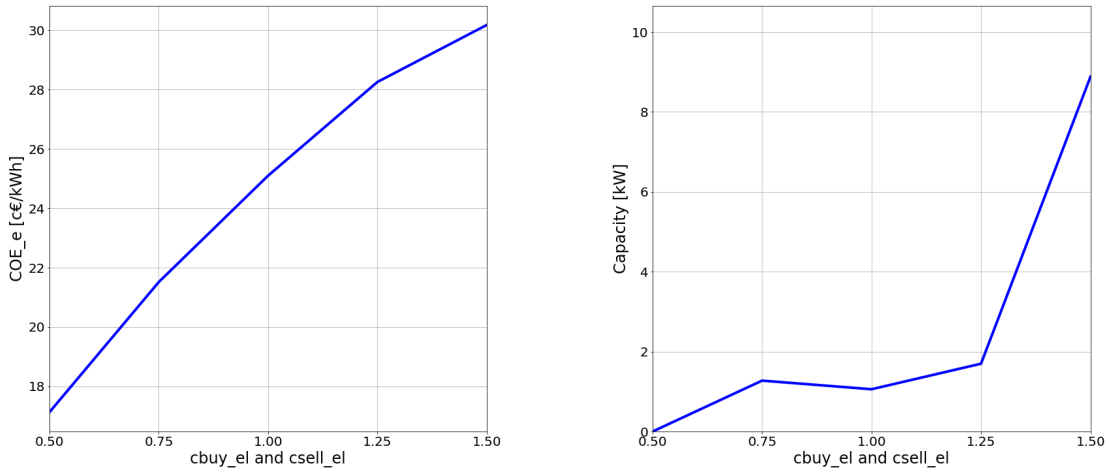

(a) (b)

Figure 40: $cbuy_{el}$ and $csell_{el}$ plot against the (a) COE_e and the (b) PV capacity

As the absolute value of the buying and selling price electricity rises, the COE increases linearly, but the PV now does not. The installed capacity stays mostly constant until after increasing of 1.25 times. Instead when the prices are halved the installed capacity is zero, as it is more convenient to just buy from the grid. The same trend can be observed in the EES.

The rest of the variables produce mostly linear relationships, so just a quick overview is produced:

- Investment costs: the COE is mostly linear and increasing, but the PV and EES capacities decrease quadratically with the investment costs.
- Interest rate, r: the COE is linear and increasing, but the PV and EES capacities decrease linearly.
- f_{sol}: the sum of $Cost_{INV}$ and $Cost_{OP}$ and the capacities are almost constant.
- h_f: the COE is linear and increasing, but the HP linearly decreases slowly.
- h_A: the COE is linear and decreasing, but the HP increases linearly and slowly.
- V_{house}: the COE is linear and increasing, but even if the HP increases linearly, the TES decreases rapidly reaching zero with a doubling of the volume.
- n_{air}: the COE is linear and increasing.
- V_{DHW}: the COE is linear and increasing.
- λ_{wall}: the COE is linear and increases rapidly with λ_{wall}.
- ρ_{wall}: the COE is mostly linear, but decreases only slightly.
- $c_{p,wall}$:the COE is mostly linear, but decreases only slightly.
- time of DHW: the COE is mostly constant, and the variable is aggregated in the total analysis of time dependent factors.
- time of occupancy: the COE is mostly constant, and the variable is aggregated in the total analysis of time dependent factors.

4) Discussion of results

During the course of this work, a model of a single household with load shifting has been developed, and in subsubsection 2.4.1 the model is first compared to two other types of simple DSM strategies. As the optimizer DR technique performs better than the other two, providing a cost for the user of 1689 $\frac{€}{yr}$ for the optimizer DR compared to 1860 $\frac{€}{yr}$ for the PBDR and to 1903 $\frac{€}{yr}$ for the IBDR, the model is therefore expanded. To reach goal number two "*Implement DSM strategies for the residential users, enabling the shifting of loads and characterize the loss of electrical and thermal comfort of the user.*" an analysis is carried out on a single household with the ability to shift three types of appliances and the ability to regulate the heating of the household. This two capabilities are limited by a threshold and symbolize the comfort levels of the user. In subsubsection 2.4.2 the analysis is laid out and in subsection 3.2 the results are shown. The critical results can be summarized with the installed capacities, for the generators respectively 2.28 kWp for the PV and 3.13 kWth for the HP. The storages are respectively 1.02 kWh for the TES and 1.41 kWh for the EES. This configuration allows for some self sufficiency (around 24% of electricity consumed is self produced), without excessive electricity selling (only around 26% of electricity produced is sold). The COE are respectively 25.83 $\frac{c€}{kWh}$ for the COE_e and 19.65 $\frac{c€}{kWh}$ for the COE_t.

As the comfort thresholds are what defines the ability of the optimizer to shift and delay the loads, a specific analysis is carried out to ascertain the effects of the change of comfort levels and, as such, fulfill goal number three "*Quantify the savings generated from the implementation of DSM and verify the correlation between savings and loss of comfort of the user.*". As the analysis is performed, a clear trend emerges from the variation of the comforts level, as both comforts show a decreasing COE as the comfort levels decrease, characterized by a rapid initial descent followed by a more gradual decline that settles at a minimum.

For the electrical comfort the start is from a COE_e of around 29 $\frac{c€}{kWh}$ and a COE_t of around 22 $\frac{c€}{kWh}$. After a sharp initial drop the chosen threshold is reached, associated with a COE_e of 25.83 $\frac{c€}{kWh}$ and a COE_t of 19.65 $\frac{c€}{kWh}$. The COE then flattens out towards a minimum of respectively 25.10$\frac{c€}{kWh}$ for the COE_e and 19.12$\frac{c€}{kWh}$ for the COE_t.

For the thermal comfort the start corresponds to a COE of around 27.2 $\frac{c€}{kWh}$ for the COE_e and 20.1 $\frac{c€}{kWh}$ for the COE_t. A more gradual decrease is observed, with the selected threshold associated with a COE_e of 25.83 $\frac{c€}{kWh}$ and a COE_t of 19.65 $\frac{c€}{kWh}$. The minimum for the COE_e is 25.7 $\frac{c€}{kWh}$, while the COE_t after reaching a minimum around 12 (with a value of 19.62 $\frac{c€}{kWh}$) trends back up, up to a value of 19.87 $\frac{c€}{kWh}$ for a comfort of 60.

Therefore, the best trade-off between savings and comfort is within the first few degrees of comfort loss and as is less convenient for the user to sacrifice all of its comfort to receive additional savings of only a few tenth of a cent per kWh.

To satisfy both the first "*Develop a model capable of simulating an energy community under constraints of optimal design and operation.*" and the fourth goal "*Evaluate the performance of the model when integrated within an EC.*" four analyses on different settings of ECs are carried out.

In the first analysis an EC of only single household with the capability of load shifting is analyzed. In the first part of the analysis all the users share the same levels of comfort. The resulting EC is observed to be a scaled version of the single household previously analyzed, as the COE remains mostly constant and the installed capacities just scale linearly with the population.

To verify whether the comfort levels play a role in this trend another analysis is carried out, with user with varying levels of comfort. When the COE is calculated for each user respectively to the consumed energy, the observed COE is higher in respect to the single household for every user.
In the second analysis, an EC comprised of household with and without load shifting is analyzed. The number of users with load shifting is set and the number of users without is instead varied. Beginning with only one user with load shifting, the emerging trend in the COE is a direct correlation with the population. As the population increases, the COE increases as well, up to a maximum of around 31 $\frac{c€}{kWh}$ for the COE_e and 23 $\frac{c€}{kWh}$ for the COE_t. The same trend can still be observed when a user with load shifting is added, even if a slight reduction in the overall cost can be observed, as the COE reaches an asymptote towards 30 $\frac{c€}{kWh}$ for the COE_e and towards 22.7 $\frac{c€}{kWh}$ for the COE_t respectively. Adding another user with load shifting produces the same trend again, with slightly lower asymptotes, around 29.7 $\frac{c€}{kWh}$ for the COE_e and around 22.5 $\frac{c€}{kWh}$ for the COE_t.
More analysis are carried out with the users being assigned the lowest level of comfort, to ascertain whether the level of comfort is instrumental to the emerging trend. For both cases with one and two users with load shifting the observable difference in COE is only of a few tenth a cent per kWh.
With this it is possible to observe that the COE is always increasing with the population, even though the addition of user with load shifting capabilities lowers the maximum reached. But this decrease slows down as more users are added and is not enough to compensate the increase in COE.
In the third analysis, the EC consists of an industrial user and a varying number of users with load shifting. As the population increases, the COE increases slightly, starting from 18.4 $\frac{c€}{kWh}$ and reaching over 19 $\frac{c€}{kWh}$ for the COE_e and starting from around 16.4 $\frac{c€}{kWh}$ and reaching around 16.55 $\frac{c€}{kWh}$ for the COE_t. The COE for this EC is lower than for the single household, but the comparison must now be made against the COE of the industrial user alone, as the loads of this user are much higher in respect to the household. The COE for the industrial user are respectively 18.23 $\frac{c€}{kWh}$ for the COE_e and 16.35 $\frac{c€}{kWh}$ for the COE_t. So for the households this EC would be convenient, but for the industrial user it would not be. Another analysis is performed with the household set to the lowest comfort level, to ascertain whether the comfort is impactful on the trend. The results show a slight decrease in COE in respect to the previous analysis, as the COE now reaches around 18.8 $\frac{c€}{kWh}$ for the COE_e and around 16.43 $\frac{c€}{kWh}$ for the COE_t. The starting values of the COE are comparable in this analysis with the case of the industrial user alone, but do not provide any real savings as the difference is in the order of a tenth of a cent per kWh.
In the fourth analysis, an EC comprised of residential users with and without load shifting and an industrial user is analyzed. The number of users with load shifting capabilities is fixed and instead the number of users without load shifting is varied. With one user with load shifting the COE presents a clear direct correlation with the population, as the COE starts respectively from around 18.5 $\frac{c€}{kWh}$ and reaches around 24 $\frac{c€}{kWh}$ for the COE_e and from around 16.5 $\frac{c€}{kWh}$ and reaches around 20 $\frac{c€}{kWh}$ for the COE_t. The COE of the industrial user alone is respectively 18.23 $\frac{c€}{kWh}$ for the COE_e and 16.35 $\frac{c€}{kWh}$ for the COE_t. Therefore, the COE of the EC is higher than for the industrial user alone.
The simulation is run again after adding another user with load shifting and the trend is almost the same, starting from and reaching almost the same values. The same is true for an EC with three users with load shifting. Then, the same process is carried out with the users set to the lowest level of comfort. The observable trend is identical as the trend

for the standard comfort level, with an overall reduction of the COE of a few tenth of a cent per kWh.
At last, to test and ascertain the degree of dependence on the assumptions made, sensitivity analyses are carried out on most of the assumed parameters.
The most interesting results are from a few parameters, such as the start time of the appliances, the solar radiation and the tariff for buying and selling the electricity.
For the start time of appliances, as the target times are set back a couple hours the COE_e reaches its maximum, with a corresponding increase in cost of around 1.8 $\frac{c€}{kWh}$. Instead, setting them forward just one hour leads to saving around 0.5 $\frac{c€}{kWh}$. Overall the dependence of the COE with the target time of the appliances is high, mostly due to the selection of a comfort level appropriate for the given start times and the ToU tariff.
For the solar radiation, the variation in COE as the solar radiation increases is negative, leading to a better result for high solar radiation. The COE_e reaches a cost of around 24 $\frac{c€}{kWh}$ for a solar radiation 1.5 times the one considered, while for lower solar radiation the COE stays the same. The main change is how the installed capacities are distributed, as the PV is strongly correlated with the solar radiation, as expected. As soon the solar radiation lowers, the capacity of the PV goes to zero, while for 1.5 times the considered solar radiation the installed capacity goes to around 11 kW, leading to negative operational costs. Instead the EES follows an opposite trend, with the capacity reaching a plateau for 0.75 and 0.5 the normal solar radiation and decreases linearly to zero for 1.5 times the considered solar radiation.
As the price of buying and selling electricity is changed together, the COE of electricity scales linearly, but the interesting effect is how the optimizer decides to distribute the installed capacities to adapt to the price difference. The PV and the EES stay pretty constant for low variations of price and instead go to zero for when the price is halved and rise up to over 8 kW for the PV and to 2.5 kWh for the EES, in respect to 2.28 kW and 1.41 kWh of the base case.

5) Conclusions

5.1 Conclusions

The model is first tested alongside two basic types of Demand Response (DR) to ascertain the potential for savings. The results indicate a reduction, specifically a 26% decrease in yearly costs for the user compared to a base case, surpassing the reduction observed with other DR types, which both reach a reduction around 18%.
Having established the economic viability and to further the development towards a complete model, a more in-depth analysis is conducted on the single residential household. The critical results can be summarized by the installed capacities. The installed generators consist of 2.28 kWp of photovoltaic (PV) panels and 3.13 kWth of heat pump (HP). The size of the PV ensures a certain degree of self-sufficiency (around 24% of electricity consumed is self produced), while also keeping the sold electricity low (only around 26% of electricity produced is sold). The HP is sized to work at the maximum load as much as possible, where it is most efficient. For the storages size are respectively 1.02 kWh for the thermal energy storage (TES) and 1.41 kWh for the electrical energy storage (EES). These storage capacities contribute to system optimization, facilitating the HP's operation at peak efficiency, mitigating exposure to high electricity prices, and providing temporal decoupling of energy demand and generation. A critical metric employed to gauge the economic performance of the model is the cost of energy (COE). The measured COE are 25.83 $\frac{c€}{kWh}$ when considering only the electrical energy used and 19.65 $\frac{c€}{kWh}$ when the thermal energy is also considered.
The comfort thresholds play a pivotal role in delineating the optimizer's capacity to shift and defer loads. To comprehend the impact of varying comfort levels, a dedicated analysis is conducted, where the user's comfort levels are varied while the COE is measured.
Both comforts achieve most of the savings in the first few degree of comfort loss, with the thermal comfort being more gradual and the electrical comfort being sharper. The standard comfort levels decided upon corresponds for the electrical comfort to a 2.4% reduction in comfort, associated with around 11% reduction in COE. Instead, for the thermal comfort a reduction in comfort of 33% to reach the standard level is associated with around 4%. It is possible to deduce that the electric comfort loss is the main driver in savings.
To review the model, sensitivity analyses are performed. Several noteworthy observations arise, the heavy dependency of the model with the time dependent variables, the solar radiation and the cost of electricity.
Subsequently the model is integrated within various energy community (EC) settings, to ascertain whether this type of user could bring additional savings to the EC. These ECs comprise of other household with load shifting, households without load shifting and an industrial user.
All the ECs analyzed exhibit a negative trend, with the COE either increasing or staying stable as users are added. This is due to the household being already optimized on its own. As such, every type of EC is at best a linear expansion of the household and at worst a worse condition for the household itself.

5.2 Future works

As the limitations of this work are apparent, several opportunities for development of the model and future research in general have been identified:

- Investigate different ToU tariffs: in the current study the ToU tariff was employed as the main driver of the time shift of energy consumptions. New ToU tariffs can be integrated in the model to change how the model responds to the optimization problem.
- Further develop the model: in the optic of modeling an EC the model could be transformed into a two stage optimization, one for the community manager to maximize the profit and one for the user to maximize the comfort. In this model the driver of the energy temporal shift could be set up as a direct payment from the community manager to the user for the comfort loss of the user.
- Test the model in different conditions: in the sensitivity analysis some geographical factors are varied, but a complete geographical comparison would certainly be interesting for this type of system.
- Include different generators and storages: the studied system is fairly simple, as to keep the results of the analyses easy to interpret. But the simplicity could be a trade off with economical advantages for the EC.
- Optimize the model: as is the model scales poorly with the number of users with load shifting. A better solution for the handling of the two comforts could be implemented, leading to the possible development of a model of an EC comprised of residential users with load shifting. With a better performing model the decreasing trend seen in the COE in the analysis of the EC of users with and without load shifting could be further investigated to ascertain the effectiveness of the EC.

With further research and development of models of ECs, to which the author hopes to have positively contributed to, more efficient and convenient systems of aggregations are being developed. Energy communities could be a crucial help in fostering a more environmentally friendly production and usage of energy.

Bibliography

[1] *The Paris Agreement*, publisher: UNFCC. [Online]. Available: https://unfccc.int/process-and-meetings/the-paris-agreement/the-paris-agreement.

[2] *Clean energy for all Europeans package*, en. [Online]. Available: https://energy.ec.europa.eu/topics/energy-strategy/clean-energy-all-europeans-package_en.

[3] *'Fit for 55': Delivering the EU's 2030 Climate Target on the way to climate neutrality*, en, 2021. [Online]. Available: https://eur-lex.europa.eu/legal-content/EN/TXT/?uri=CELEX%3A52021DC0550.

[4] *Directive (EU) 2018/2001 of the European Parliament and of the Council of 11 December 2018 on the promotion of the use of energy from renewable sources (recast) (Text with EEA relevance.)* en, Dec. 2018. [Online]. Available: http://data.europa.eu/eli/dir/2018/2001/oj/eng.

[5] I. F. Reis, I. Gonçalves, M. A. Lopes, and C. H. Antunes, "A multi-agent system approach to exploit demand-side flexibility in an energy community," en, *Utilities Policy*, vol. 67, p. 101 114, Dec. 2020, ISSN: 09571787. DOI: 10.1016/j.jup.2020.101114. [Online]. Available: https://linkinghub.elsevier.com/retrieve/pii/S0957178720301089.

[6] H. Chamandoust, S. Bahramara, and G. Derakhshan, "Day-ahead scheduling problem of smart micro-grid with high penetration of wind energy and demand side management strategies," en, *Sustainable Energy Technologies and Assessments*, vol. 40, p. 100 747, Aug. 2020, ISSN: 22131388. DOI: 10.1016/j.seta.2020.100747. [Online]. Available: https://linkinghub.elsevier.com/retrieve/pii/S2213138819309750.

[7] A. Vega, D. Amaya, F. Santamaría, and E. Rivas, "Active demand-side management strategies focused on the residential sector," en, *The Electricity Journal*, vol. 33, no. 3, p. 106 734, Apr. 2020, ISSN: 10406190. DOI: 10.1016/j.tej.2020.106734. [Online]. Available: https://linkinghub.elsevier.com/retrieve/pii/S1040619020300269

[8] E. Dal Cin, G. Carraro, G. Volpato, A. Lazzaretto, and P. Danieli, "A multi-criteria approach to optimize the design-operation of Energy Communities considering economic-environmental objectives and demand side management," en, *Energy Conversion and Management*, vol. 263, p. 115 677, Jul. 2022, ISSN: 01968904. DOI: 10.1016/j.enconman.2022.115677. [Online]. Available: https://linkinghub.elsevier.com/retrieve/pii/S0196890422004733.

[9] P. Li, Z. Wang, N. Wang, *et al.*, "Stochastic robust optimal operation of community integrated energy system based on integrated demand response," en, *International Journal of Electrical Power & Energy Systems*, vol. 128, p. 106 735, Jun. 2021, ISSN: 01420615. DOI: 10.1016/j.ijepes.2020.106735. [Online]. Available: https://linkinghub.elsevier.com/retrieve/pii/S0142061520342800.

[10] O. Alıç and Ü. B. Filik, "A multi-objective home energy management system for explicit cost-comfort analysis considering appliance category-based discomfort models and demand response programs," en, *Energy and Buildings*, vol. 240, p. 110 868, Jun. 2021, ISSN: 03787788. DOI: 10.1016/j.enbuild.2021.110868. [Online]. Available: https://linkinghub.elsevier.com/retrieve/pii/S0378778821001523.

[11] X. Yang, Z. Chen, X. Huang, R. Li, S. Xu, and C. Yang, "Robust capacity optimization methods for integrated energy systems considering demand response and thermal comfort," en, *Energy*, vol. 221, p. 119 727, Apr. 2021, ISSN: 03605442. DOI: 10.1016/j.energy.2020.119727. [Online]. Available: https://linkinghub.elsevier.com/retrieve/pii/S0360544220328346.

[12] G. Volpato, G. Carraro, M. Cont, P. Danieli, S. Rech, and A. Lazzaretto, "General guidelines for the optimal economic aggregation of prosumers in energy communities," en, *Energy*, vol. 258, p. 124 800, Nov. 2022, ISSN: 03605442. DOI: 10.1016/j.energy.2022.124800. [Online]. Available: https://linkinghub.elsevier.com/retrieve/pii/S0360544222017030.

[13] X. Fan, X. Li, Y. Ding, J. He, and M. Zhao, "Demand response scheduling algorithm for smart residential communities considering heterogeneous energy consumption," en, *Energy and Buildings*, vol. 279, p. 112 691, Jan. 2023, ISSN: 03787788. DOI: 10.1016/j.enbuild.2022.112691. [Online]. Available: https://linkinghub.elsevier.com/retrieve/pii/S0378778822008623.

[14] X. Luo and K. Fong, "Development of integrated demand and supply side management strategy of multi-energy system for residential building application," en, *Applied Energy*, vol. 242, pp. 570–587, May 2019, ISSN: 03062619. DOI: 10.1016/j.apenergy.2019.03.149. [Online]. Available: https://linkinghub.elsevier.com/retrieve/pii/S0306261919305586.

[15] L. M. P. Ghilardi, A. F. Castelli, L. Moretti, M. Morini, and E. Martelli, "Co-optimization of multi-energy system operation, district heating/cooling network and thermal comfort management for buildings," en, *Applied Energy*, vol. 302, p. 117 480, Nov. 2021, ISSN: 03062619. DOI: 10.1016/j.apenergy.2021.117480. [Online]. Available: https://linkinghub.elsevier.com/retrieve/pii/S0306261921008680.

[16] M. Safarzaei, "Comfort loss associated with automated demand response for multi-objective optimal power flow," en, *International Journal of Electrical Power & Energy Systems*, vol. 128, p. 106 672, Jun. 2021, ISSN: 01420615. DOI: 10.1016/j.ijepes.2020.106672. [Online]. Available: https://linkinghub.elsevier.com/retrieve/pii/S0142061520342174.

[17] D. Wu, G. Fan, Y. Duan, *et al.*, "Collaborative optimization method and energy-saving, carbon-abatement potential evaluation for nearly-zero energy community supply system with different scenarios," en, *Sustainable Cities and Society*, vol. 91, p. 104 428, Apr. 2023, ISSN: 22106707. DOI: 10.1016/j.scs.2023.104428. [Online]. Available: https://linkinghub.elsevier.com/retrieve/pii/S2210670723000392.

[18] G. Aruta, F. Ascione, N. Bianco, T. Iovane, M. Mastellone, and G. Maria Mauro, "Optimizing the energy transition of social housing to renewable nearly zero-energy community: The goal of sustainability," en, *Energy and Buildings*, vol. 282, p. 112 798, Mar. 2023, ISSN: 03787788. DOI: 10.1016/j.enbuild.2023.112798. [Online]. Available: https://linkinghub.elsevier.com/retrieve/pii/S0378778823000282.

[19] A. Ali Dashtaki, S. Mehdi Hakimi, Arezoo Hasankhani, G. Derakhshani, and B. Abdi, "Optimal management algorithm of microgrid connected to the distribution network considering renewable energy system uncertainties," en, *International Journal of Electrical Power & Energy Systems*, vol. 145, p. 108 633, Feb. 2023, ISSN: 01420615. DOI: 10.1016/j.ijepes.2022.108633. [Online]. Available: https://linkinghub.elsevier.com/retrieve/pii/S0142061522006299.

[20] J. Guo, P. Zhang, D. Wu, *et al.*, "Multi-objective optimization design and multi-attribute decision-making method of a distributed energy system based on nearly zero-energy community load forecasting," en, *Energy*, vol. 239, p. 122 124, Jan. 2022, ISSN: 03605442. DOI: 10.1016/j.energy.2021.122124. [Online]. Available: https://linkinghub.elsevier.com/retrieve/pii/S0360544221023720.

[21] L. Wang, J. Lin, H. Dong, Y. Wang, and M. Zeng, "Demand response comprehensive incentive mechanism-based multi-time scale optimization scheduling for park integrated energy system," en, *Energy*, vol. 270, p. 126 893, May 2023, ISSN: 03605442. DOI: 10.1016/j.energy.2023.126893. [Online]. Available: https://linkinghub.elsevier.com/retrieve/pii/S0360544223002876.

[22] Q. Lu, Q. Guo, and W. Zeng, "Optimization scheduling of integrated energy service system in community: A bi-layer optimization model considering multi-energy demand response and user satisfaction," en, *Energy*, vol. 252, p. 124 063, Aug. 2022, ISSN: 03605442. DOI: 10.1016/j.energy.2022.124063. [Online]. Available: https://linkinghub.elsevier.com/retrieve/pii/S0360544222009665.

[23] F. Issi and O. Kaplan, "The Determination of Load Profiles and Power Consumptions of Home Appliances," en, *Energies*, vol. 11, no. 3, p. 607, Mar. 2018, ISSN: 1996-1073. DOI: 10.3390/en11030607. [Online]. Available: http://www.mdpi.com/1996-1073/11/3/607.

[24] M. Rahimi and A. Sabernaeemi, "Experimental study of radiation and free convection in an enclosure with under-floor heating system," en, *Energy Conversion and Management*, vol. 52, no. 7, pp. 2752–2757, Jul. 2011, ISSN: 01968904. DOI: 10.1016/j.enconman.2011.02.020. [Online]. Available: https://linkinghub.elsevier.com/retrieve/pii/S0196890411001014.

[25] K. Kontoleon and E. Eumorfopoulou, "The influence of wall orientation and exterior surface solar absorptivity on time lag and decrement factor in the Greek region," en, *Renewable Energy*, vol. 33, no. 7, pp. 1652–1664, Jul. 2008, ISSN: 09601481. DOI: 10.1016/j.renene.2007.09.008. [Online]. Available: https://linkinghub.elsevier.com/retrieve/pii/S0960148107002844.

[26] S. Jayamaha, N. Wijeysundera, and S. Chou, "Measurement of the heat transfer coefficient for walls," en, *Building and Environment*, vol. 31, no. 5, pp. 399–407, Sep. 1996, ISSN: 03601323. DOI: 10.1016/0360-1323(96)00014-5. [Online]. Available: https://linkinghub.elsevier.com/retrieve/pii/0360132396000145.

[27] M. Frahm, F. Langner, P. Zwickel, J. Matthes, R. Mikut, and V. Hagenmeyer, "How to Derive and Implement a Minimalistic RC Model from Thermodynamics for the Control of Thermal Parameters for Assuring Thermal Comfort in Buildings," in *2022 Open Source Modelling and Simulation of Energy Systems (OSMSES)*, Aachen, Germany: IEEE, Apr. 2022, pp. 1–6, ISBN: 9781665410083. DOI: 10.1109/OSMSES54027.2022.9769134. [Online]. Available: https://ieeexplore.ieee.org/document/9769134/.

[28] *Addendum d to ANSI/ASHRAE Standard 55-2017*, en. [Online]. Available: https://www.ashrae.org/file%20library/technical%20resources/standards%20and%20guidelines/standards%20addenda/55_2017_d_20200731.pdf.